THE UNIVERSITY OF CALGARY

Forest Inventory Classification using Aerial Image Texture in the New Brunswick Acadian Forest Region

by

Alan John Maudie

A THESIS SUBMITTED TO THE
FACULTY OF GRADUATE STUDIES IN PARTIAL
FULFILLMENT OF THE REQUIREMENTS FOR THE DEGREE OF
MASTER OF SCIENCE

DEPARTMENT OF GEOGRAPHY

CALGARY, ALBERTA

JUNE, 1999

ABSTRACT

In this study a Compact Airborne Spectrographic Imager data set, acquired over the Acadian mixed-wood forest of southeastern New Brunswick, was analyzed for classification using forest cover types outlined by the New Brunswick Department of Natural Resources and Energy. Six spectral channels, and eight texture channels derived from second-order texture measures were used in classifications to determine the usefulness of including textural information in a maximum likelihood decision rule. Two separate images were classified three times using signatures generated from spectral channels alone, texture channels alone, and a combination of spectral and texture channels. Field data used to determine classification accuracies included a plot level survey of species composition by percent crown, crown closure, stems per hectare, and understory. On average, the use of texture channels in a hierarchical signature merging approach improved per-pixel classification accuracies by 28%, per-plot accuracies by 25%, and KHAT scores by 32% over classifications that used spectral channels alone. At the lower class detail end of the hierarchies an average per-pixel accuracy of 82%, per-plot accuracy of 100%, and a KHAT score of 0.78 were achieved.

ACKNOWLEDGMENTS

Without support from several people and organizations this research would have not been possible. My supervisor, Dr. Steven Franklin, contributed a substantial quantity of time and effort to this project, for which I am greatly indebted. His enthusiasm towards research and demand for independent thinking allowed me to achieve a level of understanding that I did not think was possible. Enough can not be said about Dr. Mike Lavigne of the Canadian Forest Service. he is a fine piece of work and a superior research scientist. Dr. Lavigne organized the logistics and funding for the majority of the field campaign, played an integral part in the research design, and served on the thesis committee. I would also like to give a special acknowledgment to the other members of my committee, Dr. Darren Sjogren, and Dr. Ed Johnson for providing a thorough review of my thesis.

Thanks to all of the staff and students in the Department of Geography. Special thanks to the office staff for being so kind, Monika Moskal for her input and response to my ideas, Medina Dueling for her assistance with software and hardware, and Dr. Clarence Woudsma for participating in my thesis proposal defense. Thanks to Julia Linke and Andrew Ness from UNB for providing assistance in the field. I would also like to thank Dr. Mike Wulder of the Canadian Forest Service for providing detailed answers to all of my e-mail queries, and performing the geometric and atmospheric corrections to the *casi* imagery.

The majority of the funding for this project came through scholarships from the Natural Science and Engineering Research Council of Canada and the Canadian Forest Service (NSERC supplement). Initial financial support for this thesis came from two Teaching Assistantships and a Graduate Research Scholarship supplied by the Faculty of Graduate Studies, through the Department of Geography. Last but not least I would like to thank my parents (Ken and Brenda) for bridging the financial gaps I encountered along the way as well as providing affordable housing during the duration of my thesis.

DEDICATION

To Suzanne and all of the Bombers.

TABLE OF CONTENTS

APPROVAL PAGE ii

ABSTRACT iii

ACKNOWLEDGMENTS iv

DEDICATION v

TABLE OF CONTENTS vi

LIST OF TABLES ix

LIST OF FIGURES AND PLATES x

1. OVERVIEW 1

1.1. Introduction 1

1.2. Research Objectives 5

1.3. Organization of Thesis 6

2. REMOTE SENSING OF FOREST SPECIES COMPOSITION AND STRUCTURE 7

2.1. Introduction 7

2.2. Aerial Photo Interpretation for Forest Inventory 8

2.2.1. Overview of Forest Inventory Map Production 9

2.2.2. Map Accuracies and Update Procedure 11

2.3. Digital Mapping in Forestry 13

2.3.1. Supervised Digital Classification Theory 13

2.3.2. Forest Inventory Applications of Digital Mapping 16

2.3.3. Texture Analysis Theory 22

2.3.4. Texture for Improved Classification Accuracies 29

2.4. Conclusion 30

3. STUDY AREA AND DATA COLLECTION **32**

3.1. Location and Description of Study Area 32

3.2. Data Acquisition 34

3.2.1. Compact Airborne Spectrographic Imager (casi) 35

3.2.2. Ground Based Data 38

3.3. Chapter Summary 47

4. METHODOLOGY FOR MULTISPECTRAL CLASSIFICATION USING TEXTURE **48**

4.1. Introduction 48

4.2. Classification Procedure 50

4.2.1. Creation of Normalized Difference Vegetation Index Channel 50

4.2.2. Creation of Texture Channels 51

4.2.3. Signature Generation 56

4.2.4. Classification Procedure 59

4.2.5. Classification Accuracy Assessment 60

4.3. Chapter Summary 62

5. CLASSIFICATION OF SPECIES COMPOSITION AND STRUCTURE: RESULTS AND DISCUSSION **63**

5.1. Introduction 63

5.2. Hayward Brook Image Classification Results 65

5.3. Dubee Image Classification Results 72

5.4. Discussion 77

5.5. Optimal Accuracies 83

5.6. Summary 84

6. SUMMARY AND CONCLUSIONS **85**

6.1. Summary 85

6.2. Conclusions **88**

6.3. Recommendations for Further Research 90

7. REFERENCES **92**

Appendix A **100**

Appendix B **102**

Appendix C **104**

LIST OF TABLES

Table 2.1 Classification accuracy by class for selected functions (from Franklin. 1994).....19

Table 3.1 Fundy Model Forest *casi* image channel summary.....35

Table 3.2 DNRE crown closure classes.....41

Table 4.1 Mean standard deviation of pixel values for all 48 plots used in the classification.....52

Table 4.2 Per-pixel classification accuracies from an analysis conducted to determine optimal window size for generating texture channels to be used in the classification of the Fundy Model Forest *casi* image.....54

Table 4.3 Per-pixel classification accuracies from analysis conducted to determine the optimal texture algorithms for classifying the Fundy Model Forest *casi* image 55

Table 4.4 Group classes and structure 57

Table 5.1 Listing of channel combinations used in the classification of both flight lines.....64

Table 5.2 Hayward Brook classes and structure 65

Table 5.3 a,b,c Error matrices for Hayward Brook Level 1.....67

Table 5.4 a,b,c Error matrices for Hayward Brook Level 2.....69

Table 5.5 a,b,c Error matrices for Hayward Brook Level 3.....70

Table 5.6 Dubee classes and structure.....72

Table 5.7 a,b,c Error matrices for Dubee Level 1.....74

Table 5.8 a,b,c Error matrices for Dubee Level 1.....75

Table 5.9 Optimal per-pixel classification accuracies for the Hayward Brook and Dubee images.....84

LIST OF FIGURES AND PLATES

Figure 2.1 Spectral signature generation example.....15

Figure 2.2 Textural variability inherent to forest stands 23

Figure 2.3 A simplified example of areas (referred to as plots) with different texture that produce the same spectral signature 24

Figure 2.4 Co-occurrence matrix 26

Figure 3.1 TM false color composite of study area 33

Figure 3.2 Portions of both the Hayward Brook and Dubee *casi* image.....37

Figure 3.3 Three scenarios encountered when viewing the bole of a tree through a wedge prism 39

Figure 5.1 Classification results for Hayward Brook classifications.....68

Figure 5.2 Classification results for Dubee classifications.....73

Figure 5.3 The three cases out of twenty four where the use of texture channels resulted in lower classification accuracies than using spectral channels alone.....78

Figure 5.4 Examples of where the use of texture improved classification accuracies.....79

Plate 3-1 Open canopy (low crown closure).....43

Plate 3-2 Closed canopy (high crown closure).....43

Plate 3-3 Heavy fir understory.....44

Plate 3-4 Light understory.....44

1. OVERVIEW

1.1. Introduction

Canadian forests cover 453 million ha or 45% of the country's total land base (Brand, 1990). Management level inventory systems exist for 344 million ha of the country's forests, comprised of approximately 38,000 separate map sheets and 14.4 million stands, the completion of which is primarily a provincial responsibility (Leckie and Gillis, 1995). Remote sensing of Canadian forests for surveying and management purposes began in the 1920's with the experimentation and use of aerial photographs. In the 1950's, Canada became one of the first nations to implement large area management inventories, utilizing air-photo interpretation (Leckie, 1990). In 1972, with the introduction of the Landsat satellite, remote sensing entered into the digital era and since then sensors and processing systems have improved, allowing new innovative methods for extracting forest inventory information from the data to be developed.

Although digital remote sensing methods have attained a high level of sophistication, Canadian forest inventories still rely extensively on information derived from aerial photos (Magnussen, 1997; Wulder, 1998a). Due to the cost and intensive labour involved in acquiring and interpreting aerial photographs, most provinces will only complete a full update every ten to twenty years (Leckie and Gillis, 1995). As commercial use of forests are approaching their sustainable limit, more accurate inventories are desired by forest managers at smaller, perhaps even, annual time intervals. A possible means of meeting this management objective is through the classification of high spatial resolution (pixel size $\leq$ 1 m) multispectral digital imagery (Franklin,1994; Leckie et al., 1995).

Past attempts at using satellite imagery for forest inventory have been hindered by the coarse spatial resolution of the multispectral data currently available from satellite platforms. Prior to the recent introduction of the Indian Resources Satellite-1D (IRS-1D) with a 5 x 5 m multispectral resolution, the highest multispectral resolution available from space was 10 x 10 m from the French satellite SPOT (by incorporating the panchromatic channel). While high spatial resolution data are currently available from lightweight aircraft, the aerial coverage is too small to be utilized for forest inventory. However, in the near future high spatial resolution data will be available from satellite platforms (Glackin, 1998), greatly reducing data costs and perhaps increasing the feasibility of their use in forest management inventories (Wulder 1998a). This upcoming availability of high resolution satellite imagery represents an advance in technology needed to make progress in meeting the underlying goal of forestry remote sensing outlined by Franklin (1994, page 1234): "*It is a central hypothesis of our continuing work in remote sensing of Canadian forests that stands considered distinct for inventory purposes using conventional aerial photointerpretation techniques can be separated consistently using digital classification methods.*"

Compared to the quantity of satellite remote sensing studies that have addressed forest inventory issues, a relatively small amount of research has been done using airborne high spatial resolution multispectral digital data for the purposes of mapping forests. Typically, the main goal has been to improve the classification or map accuracy to a level which meets or exceeds that currently achieved by aerial photo interpretation techniques, while at the same time retaining a class or labelling scheme with a similar level of detail to that which is currently found on forest inventory maps. Digital techniques commonly applied to meet this goal include the application of advanced methods such as automated image segmentation (e.g., Ryherd and Woodcock, 1996; Lobo, 1997), pixel un-mixing (e.g., Peddle et al., 1999), and individual tree crown delineation (e.g., Hall et al., 1998). Other studies have used

conventional classification methods, but have included the uses of ancillary data such as digital elevation models (DEMs) (e.g., Franklin, 1994). While these methods will undoubtably contribute to the successful use of high spatial resolution image analysis in forestry, there are some disadvantages. For example, they can require costly data sets such as high resolution DEMs, which are not always available and may have to be constructed. Some methods such as pixel un-mixing can require extensive field data collection coincident with the remote sensing data acquisition. In addition, most of these methods require specialized software not always commercially available to industry, and an advanced understanding of the data and software that is not common (to the average image analyst). Forest managers utilizing high resolution digital imagery in the near future will most likely continue to use commercially available software packages and the classification algorithms inherent to them. Therefore, relatively simple and cost effective techniques are desired that can improve classification accuracies while using these algorithms on high spatial resolution data.

Any object or surface cover portrayed by a digital image will be shown as a continuous surface of squares or pixels organized in a grid. Assuming a constant area, the smaller the pixel the higher the spatial resolution, and the larger the pixel the lower or coarser the resolution. Each pixel is assigned a digital number (DN), which on a monitor or hardcopy can be assigned a colour or shade of grey. The change in colour or grey scale between pixels produces a texture which is unique to that object. As the resolution of an image increases so to does the texture of the objects or cover types within it. The human eye, in conjunction with the processing abilities of the brain has an extremely advanced capability of determining or classifying objects based on their texture. For example, most people have no problem separating real grass from astro turf, even though they are both green, because these surfaces have different textures. Measuring the inherent texture of objects or cover types on digital

images and using that information as supplement to the object "colour" is a viable means of increasing the discriminatory power of digital classifiers (Mather, 1987).

In the early 1970's, with improved computer processing capabilities, authors such as Haralick et al. (1973), began work on classifying digital images, by quantifying the inherent texture of each object in the image. Studies since then have shown that texture analysis can improve the classification accuracy of digital images in a wide range of applications (e.g., Weszka, et al., 1976; Hsu, 1978; Connors and Harlow, 1980; Franklin and Peddle, 1987; Marceau et al., 1990). However, studies which used satellite imagery were hindered by their low resolution, and were forced to classify large areas in order to produce enough texture to make analysis of it useful. Subsequently, these areas were too large to compete with the detail of the forestry stand maps produced by aerial photo interpretation. With the current availability of high resolution multispectral imagery from airborne platforms, and in the very near future from satellite platforms, the usefulness of texture analysis in the classification of high resolution imagery, for the purposes of forest inventory, has become a topic worthy of continued study. Earlier efforts (e.g., Franklin and McDermid, 1993; Wulder et al., 1996a; Lobo,1997; St-Onge and Cavayas, 1997; Bruniquel-Pinel and Gastellu-Etchegorry, 1998) have shown the value of texture in specific applications, however the use of high resolution texture analysis in digital forest inventory classifications has not been adequately addressed.

1.2. Research Objectives

The objective of this thesis is to expand and improve upon previously completed work (Franklin et al., in press) involving the classification of forest species on high resolution multispectral images, while utilizing a standard, commonly available, texture analysis procedure. The two central objectives of this research are:

(i) To show that high spatial resolution multispectral imagery can be classified using forest inventory classes outlined by the New Brunswick Integrated Land Classification System (New Brunswick Department of Natural Resources and Energy, 1996);

(ii) To show the extent to which the inclusion of textural information derived from readily available (second-order) texture measures in a maximum likelihood classifier will improve classification accuracies.

1.3. Organization of Thesis

This thesis is organized into six chapters. Chapter one introduced the topic of remote sensing for improved forest inventory, and the concept of texture analysis, which is the central theme of this thesis. Chapter one also outlined the objectives for a test of aerial image texture analysis in the classification of New Brunswick forest stands in accordance to a standard forest inventory scheme.

Chapter two reviews the literature relevant to the subject of remote sensing of forest species composition, and texture analysis. This includes a review of how Canadian forests are currently mapped, general image classification theory, several previous digital mapping projects in forestry, and image texture theory. Chapter two also provides some examples of the way in which texture analysis has been used in forest inventory mapping.

Chapter three describes the New Brunswick study area and both the field and aerial digital multispectral data sets. This chapter also describes the methods used to collect the field data set and prepare it for use in the image processing and classification. Chapter four outlines the methods used to classify the digital imagery and assess classification accuracy, and reviews the selected texture analysis procedure. Chapter five reviews the significant results of the classifications and reports on the accuracies achieved.

Chapter six contains the thesis summary and conclusions as well as recommendations for further research in mapping of forest species using high resolution multispectral digital imagery.

2. REMOTE SENSING OF FOREST SPECIES COMPOSITION AND STRUCTURE

2.1. Introduction

Forest cover plays a complex role in various processes at the lithosphere-biosphere-atmosphere interface. The ability to map forest cover from remote platforms with detail, accuracy, and speed is desired by forest managers, and others, such as Global Climatic Modelers for the improved information it would contribute (Waring et al., 1986). This chapter presents a literature review that focuses on the topic of mapping forest species composition for forest inventory purposes. Progress of this subject is also important to those who wish to incorporate detailed forest cover information into their own research.

Five topics are considered in this literature review:

1) current operational methodology for collecting forest inventory data;
2) digital image classification theory;
3) digital image mapping in forestry;
4) image texture analysis theory;
5) image texture analysis for forest inventory.

A vast amount of literature exists for the first four topics and a extensive review of all aspects of this literature would be beyond the scope of this thesis. Rather, the purpose of this chapter is to show why new strategies are needed for collecting forest inventory, and why these new strategies might rely on or need improved methods for classifying high resolution digital imagery. The fifth topic (texture analysis for forest inventory) has received moderate coverage in the literature, and select examples will be reviewed. The focus of the fifth topic will be to provide examples of the way in which texture has been used for mapping both high and low resolution imagery.

2.2. Aerial Photo Interpretation For Forest Inventory

Forest inventory in Canada is primarily a provincial responsibility which is combined nationally to provide a complete perspective on the status of forest resources in Canada (Natural Resources Canada, 1997). The broad goal of forest inventory is to collect forest resource data which may include: composition, structure, condition, location, extent, and volume. Forest inventories can range in scope from operational-level inventories which focus on a small area and typically include ground based timber cruising, to management inventories which consist of complete-coverage stand mapping (Leckie and Gillis, 1995). Today, the vast majority of Canadian forest management inventory is conducted using traditional aerial photo interpretation methods (Magnussen, 1997).

The end product of most forest management inventory is a map comprised of stands (polygons on the map) considered to contain a homogeneous area (or acceptable levels of heterogeneity) of forest composition, structure, and condition (age, health, etc...). In the 1980's, most Canadian forest inventories were transferred to the digital realm of geographic information systems (GIS), however the methodology used to produce the inventory information that goes into the GIS database has remained relatively unchanged (Leckie and Gillis, 1995).

2.2.1. Overview of Forest Inventory Map Production

For simplification, the province of New Brunswick will be used as an example of the procedure for map production. Information on forest inventory map production in any other province or territory can be found in Leckie and Gillis (1995). The first stage of forest inventory map production requires the collection of aerial photos corresponding to the region to be mapped. In New Brunswick, normal color air photos are acquired at a scale of 1:12,500 for seven million hectares of forested land per inventory (approximately 37,000 photos) (Leckie and Gillis, 1995).

Stereo prints of the air photos are used by photo interpreters to delineate forest stands on the basis of homogeneous species, density, height, and age characteristics. In New Brunswick, forest stands are labeled using the New Brunswick Integrated Land Classification System (New Brunswick Department of Natural Resources and Energy, 1996), and are broken down in to three forest stand types (FST):

Forest Stand Type 1 - productive forest land with no or minimal (occupying < 30% of the stand area) unmerchantable component

Forest Stand Type 2 - productive forest land containing a merchantable overstory and a unmerchantable understory. The unmerchantable component must occupy at least 30% of the stand area and the volume of the merchantable component must be greater than 35 m^3/ha

Forest Stand Type 3 - Productive forest land with no or minimal (< 35 m^3/ha) merchantable stand component

For areas in a FST1, or the merchantable overstory of FST2, a site is described by: species composition, species specific age class, development stage of each species within the classification, percent ratio of merchantable volume of each species class component, development stage of site as a whole, horizontal stand structure (i.e., crown closure), vertical stand structure (i.e., number of canopy layers), density of merchantable stems, size (i.e., diameter at breast height) class of most merchantable volume, site indicator (e.g., soil characteristics), harvest indicator, and a silviculture indicator. The unmerchantable understory component of FST2 and unmerchantable FST3 are defined separately and in a similar fashion to the merchantable component. However, the scale and type of description is different in the unmerchantable component to allow for the description of regrowth and replanted areas (e.g., species specific age class has been replaced by an average height class ranging from 0 to >7 m).

While the above list of possible descriptors for a stand is quite extensive, the stand labels found on the maps produced from aerial photo interpretation will typically only contain the species composition, crown closure, and age class (e.g., mature, regenerating). Hardwood species composition is usually given in groupings such as intolerant hardwood (IH), or tolerant hardwood (TH), but softwood species are more often reported separately. When softwood species can not be separated or make up less than 30% of the stand they are usually reported as softwood (SW) or spruce / fir (SF).

In New Brunswick, once the photos have been interpreted, the stand boundaries (marked on the photo) are optically transferred in ink or pencil to a mylar base map, using a vertical

sketchmaster. Stand boundaries are then digitized off the base map into the GIS (in Alberta the stand boundaries are digitized directly off interpreted 1:20,000 orthophotos, eliminating one stage of the transfer). Digitizing is done manually with a high density level to maintain the original smoothness of the stand boundaries. In New Brunswick, this meant 1880 separate map sheets, each covering 4300 ha, were digitized for the last inventory.

The New Brunswick forest inventory is completed on a ten year cycle. The last inventory began in 1981 and was completed in 1986. In 1993, aerial photos were obtained, initiating the next inventory. Aerial photo coverage for New Brunswick is estimated to cost $1.15 million, and interpretation of those photos costs approximately $630,000. Transfer and drafting costs $490,000, and digitizing costs $266,000, for a total inventory mapping cost of $2.54 million. This total does not include the cost of hardware, accuracy assessment, field work, or base maps, which in the case of New Brunswick is estimated to add another $3.29 million to the overall cost (Leckie and Gillis, 1995).

2.2.2. Map Accuracies and Update Procedure

There are two types of accuracies that a map can be tested for, namely spatial and aspatial. The accuracy of a stand can also be reported both spatially and aspatially. Aspatial accuracy of a stand is directly related to the accuracy of aerial photo interpretation. Rigorous assessment of interpretation accuracy is difficult. Leckie and Gillis (1995) reported that for species composition the correct order of dominant species or species groups is 80% to 85% correct, however this is only the order, not species proportions of a stand. They state that (page 80) *"a best estimate of species accuracy is that 70% to 85% of the time the species composition is interpreted in the correct order or to within $\pm$ 25% of the true species proportion for a stand"*. High accuracies are likely achieved in pure softwood stands but most likely drop significantly in mixed-wood or complex hardwood stands. The spatial

accuracy of stand boundaries is also subject to different means of accuracy assessment. Those stands which border a feature of known location, such as a road or river are very accurate. Accuracy of stand boundaries that do not border any obvious feature becomes an issue when one compares the location and extent of a boundary interpreted at different times (i.e., comparing a stand from the 1980 inventory to the 1990 inventory). Edwards and Lowell (1995) reported a disagreement as high as 40% to 50% when maps produced at different times were overlaid.

In the 1980's, with the adoption of GIS, one of the biggest advantages promised was the ability to update an already existing forest inventory of changes to the database. For example, the extent and location of a cut-over could be transferred to the database. However, today, while cut-overs and other partial cuts are maintained as separate layers in the database and transferred from one inventory to the next, the disagreement between non-harvested stand boundaries is still too great to permit direct transferring to the "updated" inventory.

> *When a forestry database is "updated", the existing information is discarded completely. The new forest data supersede the previous data completely. Thus the "update" is not an update at all; it is the creation of a completely new database having all of the information and characteristics of the previous database. But the new forest inventory is planned and conducted using new maps produced from new aerial photographs without reference to the "outdated" forest data.* - (Lowell and Edwards, 1996, page 429)

While it is clear that the current method of producing forest inventory maps is not optimal, it should be stressed that forest management in Canada still relies extensively on information derived from aerial photo interpretation, as it is the only method currently available that is

considered economically and logistically feasible by the forest management community.

2.3. Digital Mapping in Forestry

Mapping and collecting inventory of Canadian forests from satellite platforms has been a highly studied topic since the first Landsat satellite images became available in 1972. The purpose of this section is to provide some background in digital mapping theory within the context of forestry remote sensing, while reviewing the previous research done in this topic area. The idea is to provide an understanding of the context and significance of the research objectives outlined in section 1.2 (page 5).

2.3.1. Supervised Digital Classification Theory

Digital images are composed of pixels organized in a grid of lines and rows. Each pixel has a value (color or shade of grey) that represents the real world object being depicted. Multispectral images combine multiple images (spectral channels) acquired at different wavelengths to make up one image. A normal color image combines spectral channels in the blue (0.4-0.5 nm), green (0.5-0.6 nm), and red (0.6-0.7 nm) wavelengths to produce an image that looks the same as the human eye sees the real world. However, if the blue spectral channel is replace by a near infrared spectral channel (0.7-0.9 nm), the image would appear false because the human eye cannot see infrared light. The resulting "false color" image is useful for discriminating between vegetation types. For example, the false color composite described above would produce green colors for needle bearing trees, and red to pink colors for leaf bearing trees, making delineation between the two much easier than on a normal color image.

A supervised classification (user defined classes) of an image requires that the image analyst knows the spectral value of the pixels that make up each class, for each wavelength. Once

the spectral values for an object are known, all other pixels with similar values can be automatically assigned the same class. This process usually involves four logical steps:

1) areas of known cover type are identified and given a class label;
2) a "spectral signature" is generated for each known cover type or class;
3) the image is "classified" using the spectral signatures as reference to determine the class of all pixels on the image;
4) the accuracy of the classification is assessed in areas of known cover type.

Simply expressed, a spectral signature is a collection of statistics derived from the pixel values of a "training area". Typically, the spectral signature of a training area is the mean and standard deviation of pixel values for each spectral channel within that area. To determine the spectral signature for an object or cover type a spectral signature is generated in the area(s) that coincide(s) to that object. Figure 2.1 gives an example of how a spectral signature is generated for a 5 x 5 pixel forested area. Once the spectral signature is generated it is used in the classification stage as the reference for that class.

Most classifiers found in commercial software are statistical classifiers. Statistical classifiers compare each pixel in the image to the statistical properties of the spectral signatures to determine that pixel's class. Classifiers can range in complexity from simple linear classifiers, such as the Minimum Distance to Means classifier, to those that incorporate Fuzzy Logic. Arguably the most common statistical classifier is one that utilizes a Maximum Likelihood decision rule. Maximum Likelihood classifiers calculate the probability of a pixel belonging to each class and then assigns the pixel to the class of highest probability. In doing this the Maximum Likelihood classifier makes an assumption that the training statistics are normally distributed (Gaussian). Violations of this assumption usually result in reduced classification accuracies (Strahler, 1980).

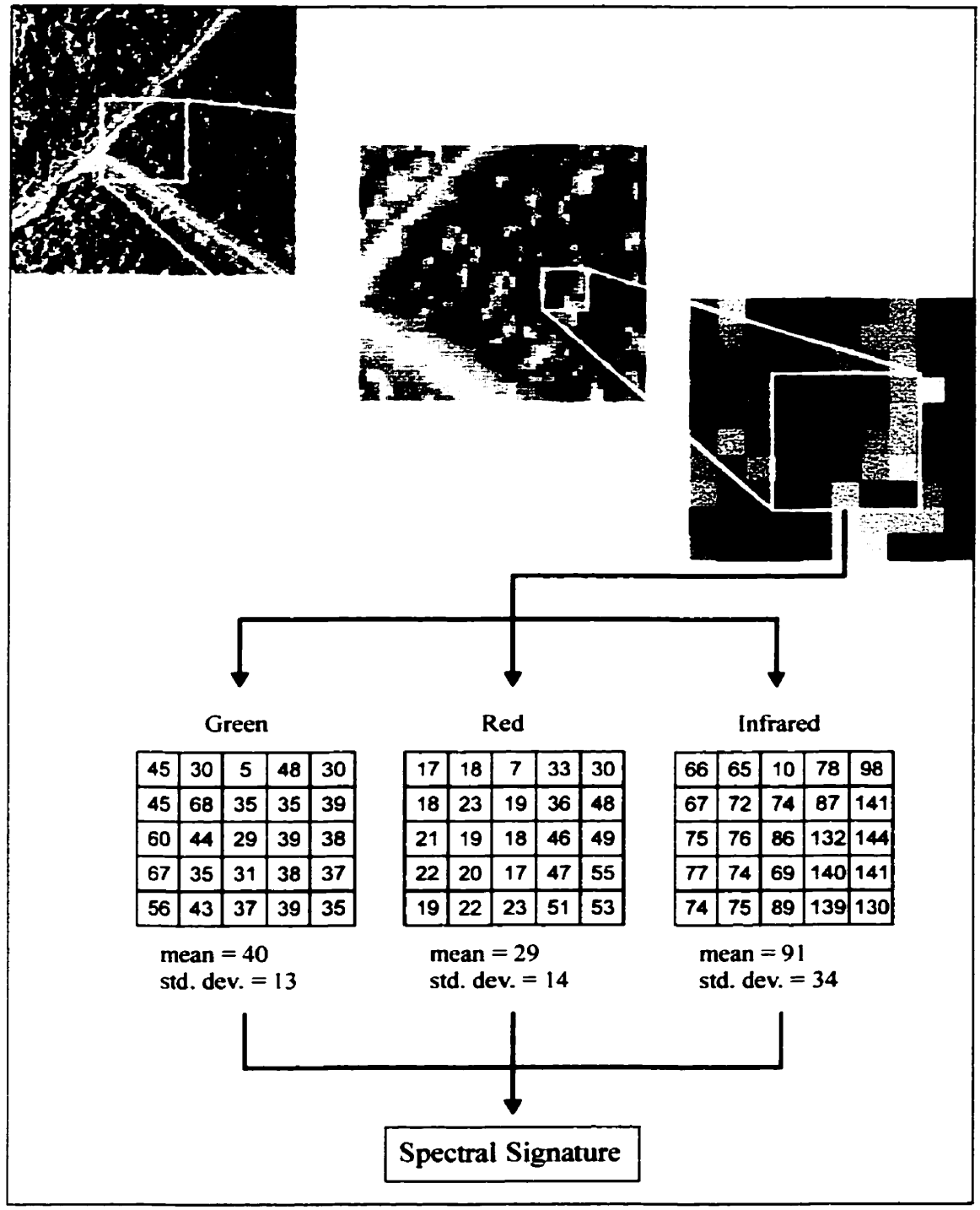

Figure 2.1 Spectral signature generation example for an area of 5 x 5 pixels. The imagery is displayed as a false color composite wherein all three channels are displayed at the same time, but are actually maintained seperately in the database (i.e., each pixel displayed has three values).

Although it is quite often overlooked, the most important stage of any classification is the accuracy assessment, because it allows map users to evaluate the data quality of the map and identify if it is suitable for their intended application (Stehman and Czaplewski, 1998). "*A classification is not complete until its accuracy is assessed*" (Lillesand and Kiefer, 1994, page 612). Classification accuracies are usually assessed in a per pixel manner. For example, if 97 pixels are classified as water in a 100 pixel area known to be water, the per pixel classification accuracy for water would be reported as 97%. A properly executed classification will use separate ground truth areas for training and assessing classification accuracy. While assessing the classification accuracy of training areas can provide valuable information regarding the spectral separability of the signatures used, they should not be reported as an indication of overall accuracy as they may produce favorable results (Lillesand and Kiefer, 1994).

2.3.2. Forest Inventory Applications of Digital Mapping

Initial studies utilizing digital mapping techniques for forest inventory relied heavily on satellite imagery. The large swath width or aerial coverage of satellite images made proposed inventories from them economically attractive. Until the recent availability of 5 x 5 m multispectral digital imagery from the Indian satellite IRS, the highest spatial resolution multispectral image available from space was 20 x 20 m, obtained from the French satellite SPOT (Systeme probatoire d'observation de la Terre), which was launched in 1986. Prior to this the Landsat Thematic Mapper (TM) was launched in 1982, with a spatial resolution of 30 x 30 m. Its predecessor was the Landsat Multispectral Scanner (MSS), with a spatial resolution of 79 x 79 m, launched in 1972. Many studies have utilized these satellite images for forest inventory mapping (e.g., Beaubien, 1979; Bryant et al., 1980; Walsh, 1980; Teillet et al., 1981; Cognalton et al., 1983; Nelson et al., 1984; Benson & DeGloria, 1985; Horler and Ahern, 1986; Williams and Nelson, 1986; Cibula and Nyquist, 1987; Hudson, 1987; Hopkins et al., 1988; Franklin and Peddle, 1990; Marceau et al., 1990; Ghitter et al., 1995; Sader et al., 1995).

The majority of these studies used classes that were anticipated to produce spectral signatures that were separable. That is, classes were selected based on the distinctiveness from above, as opposed to those driven by the needs of forest managers. This has generated the single biggest criticism of satellite remote sensing for forest inventory purposes; poor spatial resolution has resulted in classification schemes that are far too coarse for meaningful forest management planning at the stand level (Leckie, 1990). For example, Holmgren and Thuresson (1998) point out that most of the stands that are slated to be harvested in the coming decade would fall into one class if the class scheme of many of these studies were used. As a result, a minimal contribution to the forest management decision process is gained through the majority of the satellite forest inventory projects that have attempted to map species composition, because of their failure to duplicate the detail of classes found in stand level inventories.

The limitations of low spatial resolution data acquired from satellites, prompted digital remote sensing research to construct high resolution multispectral sensors that could be mounted to light weight aircraft. Due to the sensors relative proximity to the earth the spatial resolution is greatly increased, however the extensive spatial coverage is sacrificed. At the moment, the poor spatial coverage of most high resolution airborne digital sensors is too small for practical use in forest inventory. However, these aerial data can be used to develop high resolution digital analysis methods. In the near future, high spatial resolution multispectral images will be available from space, increasing their spatial coverage, which will subsequently put high spatial resolution image analysis methods in higher demand.

Various forest attributes have been estimated using high resolution aerial digital imagery. For example, Wulder et al. (1996a) improved the estimation of leaf area index (a dimensionless index used to quantify the single sided vegetation leaf area per unit of ground area) using

digital methods applied to *casi* (Compact Airborne Spectrographic Imager) imagery. Niemann (1995) attempted to predict stand age with *casi* data based on the spectral response curve. Franklin et al. (1995) used aerial videographic data to estimate Western Spruce budworm defoliation at the scale of individual tree crowns or small stands not detected by lower resolution satellite imagery.

Other studies have focused on estimating species composition using aerial digital imagery. For example, in an attempt to increase classification accuracy using existing and straight forward methods, Gerylo et al. (1998) implemented a hierarchical decision process where classes were successively merged into broader classes, eliminated, or accepted. This process resulted in an improvement of overall average classification accuracy from 21% in level 1 to 65% in level 4, using high resolution (0.3m) aerial digital frame camera imagery. The disadvantage of this procedure is that classes become successively broader or all together eliminated resulting in a very coarse class resolution (similar to that achieved with satellite imagery) at the final level of the hierarchy.

Another means of improving the classification accuracy of species composition is to include ancillary data, such as a digital elevation model, into the classification procedure. For each class DEM data are added to the decision rule, resulting in increased class separability, which typically translates into increased classification accuracies. Franklin (1994), implemented a DEM in the discrimination of subalpine forest species and canopy density using digital airborne *casi* and satellite based data. This study showed that the classification accuracy of *casi* imagery could be improved an average of 10% for forest classes by including information supplemental to the spectral data in the classification procedure (see Table 2.1).

Table 2.1 Classification accuracy by class for selected functions (from Franklin, 1994)

	Percent Classified into Class*										
Function	1	2	3	4	5	6	7	8	9	10	11
CASI	100	93	73	60	100	67	87	47	93	93	67
DEM	73	47	60	0	33	43	57	33	67	93	0
CASI & DEM	100	93	87	73	97	77	93	73	87	100	87

*Class descriptions as follows

Class	Description	Density (%)
1	Cultural	-
2	Grassland	-
3	Aspen & Balsam Poplar	51-70
4	White Spruce & Balsam Poplar	51-70
5	Aspen and White Spruce	51-70
6	White Spruce and Aspen	51-70
7	Pine and White Spruce	51-70
8	Pine and White Spruce	71-100
9	Pine	71-100
10	Pine	6-30
11	Pine, White Spruce & Aspen	71-100

Generally speaking, the spectral response for any one forestry site is the sum of the light reflected by the trees and the ground, whether it is bare or vegetated. Therefore, sites with the same species composition and differing density will have slightly different spectral responses depending on the role the ground cover plays. This allows for the estimation of density or crown closure to accompany species composition. Franklin's (1994) study incorporated density and height into the class descriptions (e.g., there were two pine/white spruce classes, one with a density of 51-70% and the other with a density of 71-100%). The success of this can be seen in Table 2.1 where class 9 (pine) was classified at 100% and class 10 (also pine) at 87%, showing the classifier could discriminate between the two density classes with the same species composition.

Several studies have demonstrated that as spatial resolution increases, classification accuracy decreases (e.g., Irons et al., 1985; Woodcock and Strahler, 1987). Although this seems contradictory to what one would predict, these studies have shown that as spatial resolution increases so to does within class variance. This decreases the spectral separability of classes and results in lower classification accuracies (Woodcock and Strahler, 1987).

> *One of the challenges in using high-spatial resolution remotely sensed imagery for classification is termed the H-resolution problem, and implies that as the spatial resolution of a sensor increases, so does the interclass spectral variability of surface features, resulting in a reduction of statistical separability with traditional classifiers and a consequent reduction in classification accuracy.* - (Hay et al., 1995, page 110)

Irons et al. (1985) used a TM image (30 m resolution) and a degraded TM image (80 m resolution) to examine the performance of a per pixel, maximum-likelihood classification algorithm. Their study revealed findings similar to Woodcock and Strahler (1987) in that an increase in spatial resolution from 80 to 30 m caused an average of 6% decrease in accuracy. Irons et al. (1985) concluded that these findings point to a need for improved methods of classification when using successively higher resolution data, such as including textural information into the classification decision rule. Although these studies used low resolution satellite imagery (Woodcock and Strahler actually used simulated TM and MSS data), the conclusions from them hold true when the spatial resolution of high resolution data is increased. For example, Franklin et al. (in press) determined the classification accuracy of digital frame camera imagery acquired at six different altitudes, resulting in a range of spatial resolutions from 0.3 m - 8 m. They concluded that classification of the highest spatial resolution imagery produced the lowest accuracies, however they still provide the greatest amount of detail.

One current research idea for increasing the classification accuracy of forest cover, while dealing with the problem of increased scene variance, is through individually delineated tree crown classifications. Gougeon (1995) used high resolution (0.36 m) Multi-detector Electro-optical Imaging Scanner (MEIS) imagery to delineate individual tree crowns. Instead of using the entire forest stand (includes sunlight portion of crown area, shadowed portion of crown area, shadow cast by the tree, and ground cover) for deriving training statistics, only the multispectral image data from the crown (sunlight and shadowed portions) of single trees were included. This eliminated what is often referred to as "scene noise" from the classification decision rule, resulting in increased class separability and increased classification accuracies. However, this was done at the expense of manually delineating individual tree crowns in the training procedure, which is time consuming and makes this procedure unattractive to industry until automated procedures are available. Meyer et al. (1996) applied a similar technique to synthesized high resolution multispectral imagery created from digitized color infrared-aerial photographs. This again involved the manual digitization of tree crowns, but none the less improved classification 23% over classifications using an entire area for training.

There are obviously many solutions that could be used to address the requirement of increasing the classification accuracy of high spatial resolution aerial imagery. The merging of classes, inclusion of ancillary data, or the delineation of individual tree crowns, are some of the current trends in remote sensing applications to forest inventory, with the focus of improving the classification accuracy of species composition. Another alternative is the inclusion of textural information in the classification decision rule. As opposed to individual tree crown delineation methods which attempt to reduce scene variance from the decision rule, texture analysis measures this scene variance and utilizes it as information in the classification process.

2.3.3. Texture Analysis Theory

Traditionally, texture has been defined as the spatial variation in image tones or colors (Haralick et al., 1973), which in images of forest cover may be caused by changes in species type, crown closure, and/or stem density. Figure 2.2 shows several examples of the way in which texture can vary within a forest. Group 1 is an example showing that different stem densities can create different texture patterns even though they have the same species composition. Group 1A is a mature spruce stand with 500 stems per hectare, Group 1B is a spruce plantation with approximately 3000 stems per hectare. Group 2 shows the difference between two hardwood stands with different crown closures. Group 2A is a mature intolerant hardwood stand with a crown that is 70-90 % closed (i.e., looking up from below 70-90 % of the sky will be obscured by foliage). Group 2B has a much more open crown with a closure of 30-50 %. The open crown of 2B creates a larger shadow component than that seen on 2A, resulting in different textures. Group 3 shows two examples of mixed-wood stands. Group 3A is 70% hardwood and 30% softwood, as where Group 3B is 60% softwood and 40% hardwood. They both have similar structures (i.e., shadow component is similar), however their textures are different because they have different combinations of species, resulting in different variations in tone.

The calculation of image texture provides a quantification of the spatial variability of scene elements (Wulder, 1996). In the previous section, methods for minimizing scene variance (for example, tree crown delineation) were described, but the use of texture presents an almost completely opposite logic in that it utilizes this variance in the classification procedure. Measuring the texture of an image and including it with the spectral information in the classification has been shown to increase class separability and therefore classification accuracy (e.g. Franklin and Peddle, 1990; Ryherd and Woodcock, 1996; Franklin et al., in press).

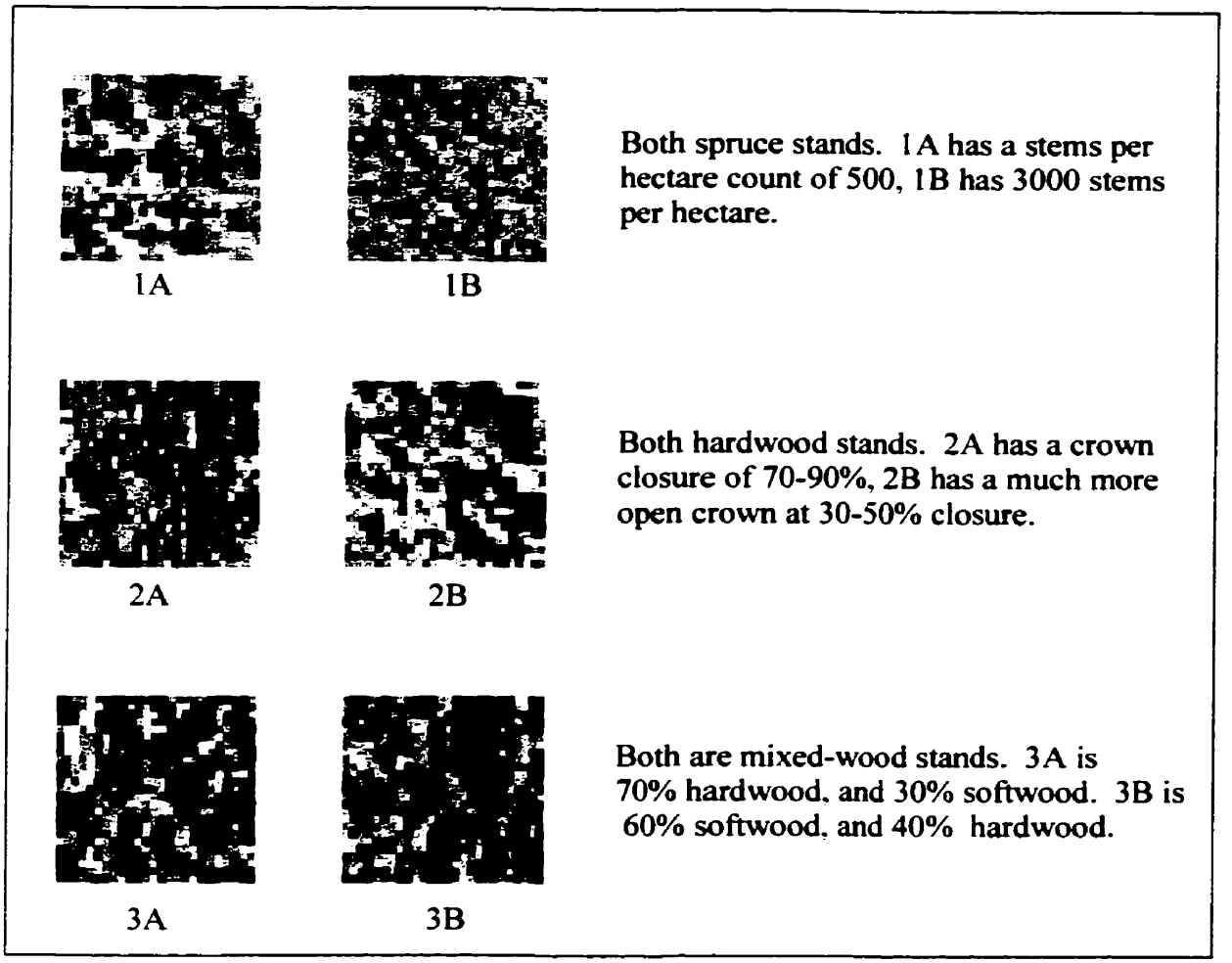

Figure 2.2 Textural variability inherent to forest stands. Group 1 shows that two stands with the same species composition can have different textures caused by different stem densities. Group 2 gives an example of how crown closure and the resulting shadow component, can cause different texture patterns. Group 3 shows that differences in species composition result in variation in color, which is essentially texture.

Figure 2.3 gives an example of very different looking (texturally speaking) stands that have the same spectral signature. Earlier, Figure 2.1 (page 15) demonstrated the way in which a

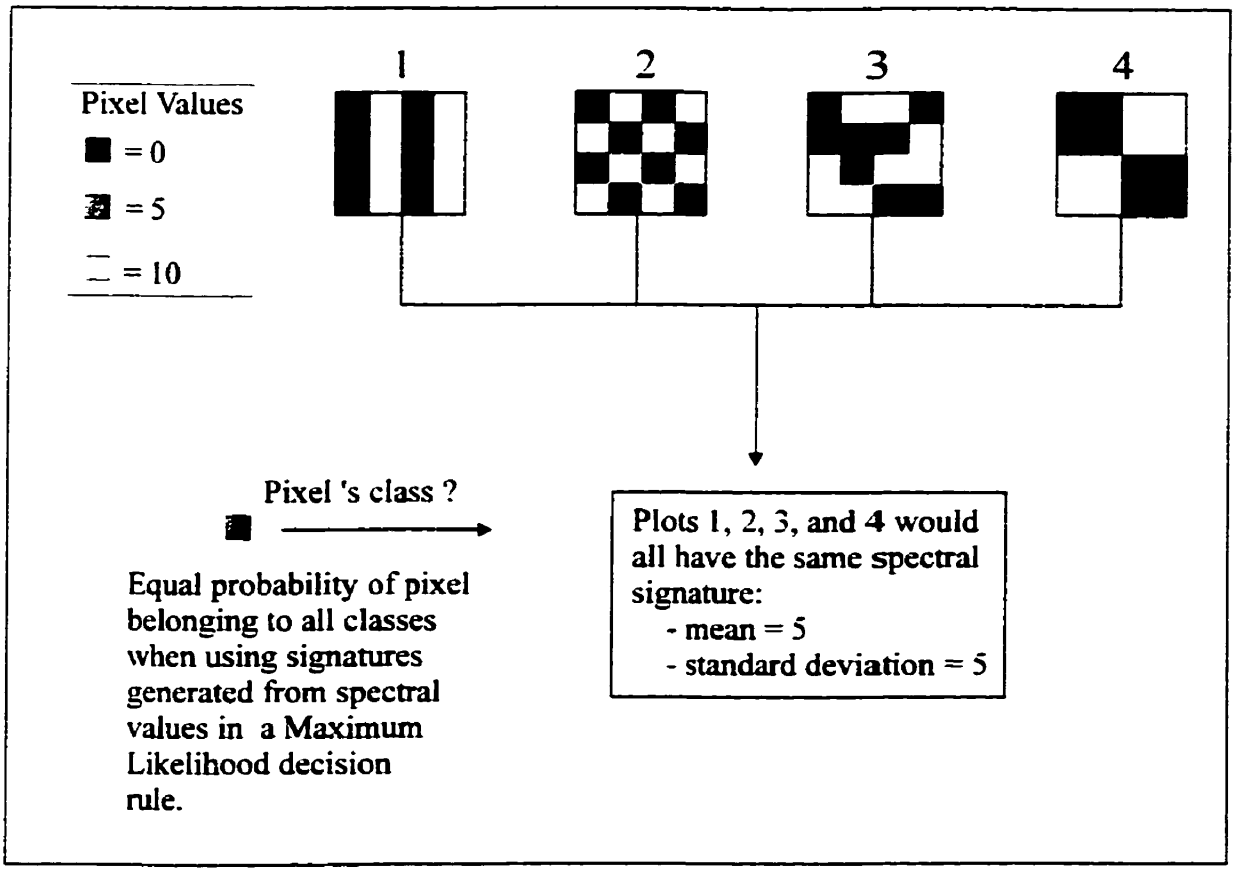

Figure 2.3 A simplified example of areas (referred to as plots) with different texture that produce the same spectral signature.

spectral signature is generated using conventional classification methodology. Essentially, a spectral signature is the mean and standard deviation of the pixel values for an assigned training area. Although the scenario shown in Figure 2.3 is a simplified example using only one spectral channel, it does show that spectral signatures generated from what the user may think are very different looking stands, can actually be spectrally identical. The logic behind texture analysis is that the different texture patterns in Figure 2.3 can be measured and used in the classification procedure as a supplement to the spectral information or on their own.

The inclusion of texture derivatives in the classification procedure is an attractive solution to increasing classification accuracy because they are supplemental to the image data, and represent an accessible, low cost (other additional information sources, such as DEMs, can be expensive to acquire due to their labor intensive construction needs), additional information source (Wulder, 1996).

Texture can be described by a variety of statistics which characterize the relationship between neighboring pixels relating to image properties of an area (Wulder, 1996). Of the various methods of measuring texture that exist, primary and secondary texture derivatives are most commonly used. Primary or first-order texture measures are derived by passing a moving window of pixels over the image for which a statistical value for the central pixel is calculated (Wulder, 1996). A new image is created from all of the values calculated for central the pixel of the window. Typical first-order statistics used are: minimum reflectance within the window, maximum reflectance within the window, range (min-max) of reflectance values, mean reflectance within the window, and standard deviation within the window. The window size used is of great importance and will be discussed later.

A more powerful means of measuring texture is through the use of secondary texture measures, which are indirect measures of the spatial variation in image tones. These may be computed from a grey level co-occurrence matrix (GLCM) defined by Haralick (1979) as a matrix of relative frequencies in which two neighboring pixels, separated by distance *d* and angle a, occur within a fixed sized moving window, one with grey tone *i*, and the other with grey tone *j*. For the following example (Figure 2.4), a co-occurrence matrix has been produced using a distance of 1 (pixel immediately next to itself) and an angle of 0 (vertical), within a 5x5 pixel window.

Window of Imagery

4	6	8	5	4
5	5	8	7	6
6	7	7	7	9
8	8	4	8	6
9	8	9	5	6

Resulting co-occurrence matrix

Neighboring pixel value

Ref. Pixel	4	5	6	7	8	9
4	0	1	1	0	0	1
5	0	0	1	2	0	0
6	0	1	1	0	1	1
7	1	0	0	1	2	0
8	0	1	0	1	2	1
9	0	0	1	0	0	0

Figure 2.4 Example of a co-occurrence matrix (from PCI Inc. EASI/PACE, 1997).

In this example the program begins in the top left corner and counts the occurrences of a reference pixel with a value of four occurring above or below a neighboring pixel of five. This only occurs once as can be seen in the co-occurrence matrix. From the GLCM, statistics such as homogeneity, contrast, dissimilarity, mean, variance, entropy, and angular second moment may be calculated using image processing software (for equations see sections 4.2.2.) (PCI, 1997). Secondary texture derivatives are available for use in commercial software packages and the results are written to individual channels, which can then be treated as an additional channel for inclusion in signature generation and classification.

A third means of measuring texture is through the use of a spatial autocorrelation function, such as the semivariogram (Carr and Pelon de Miranda, 1998). A simplified explanation of semivariance is that it produces a graphical representation of the spatial variability of reflectance values surrounding a pixel. The semivariance profile of a user defined area or site is essentially the texture descriptor for that area. St-Onge and Cavayas (1995) used semivariance to estimate the stocking and height of forest stands. Wulder (1996), applied

semivariance analysis to *casi* imagery with the intent of developing a relationship between texture and leaf area index (LAI), which can be used to estimate forest stand net primary productivity (NPP). Semivariance can also be used to predict the optimal geographic window size to be used in other image analysis or with first and second-order texture measures (e.g., Franklin et al., 1996). Semivariance image analysis is complex and requires specialized software typically written in high level code.

Regardless of the actual measure, texture analysis requires the analyst to consider a large suite of variables. The user can choose which texture measure to use, which algorithms within that measure, the window size or area to be analyzed, in the case of second order and semivariance the direction in which to measure, the spectral channel(s) to measure, and even the quantization level (8-bit, 16-bit, or 32-bit).

Over the last twenty years a large number of studies using everything from simulated images to satellite imagery have concluded that second-order texture measures will usually out perform first-order measures in terms of classification accuracy or pattern recognition (Marceau et al., 1990). The reason for this is that they are based on a better statistical description of the image than first-order statistics, because in addition to a statistical description of grey-level distribution they also describe the relationship between neighboring pixels. However, few comparisons between these more traditional second-order texture measures and more recently derived semivariance measures have been conducted with the goal of determining which measure will improve classification accuracies the most. A recent study by Carr and Pelon de Miranda (1998) found that semivariance produced the best accuracies when classifying microwave images and that second-order measures produced superior accuracies when classifying optical imagery. These findings combined with the availability of second-order analysis over that of semivariance suggests that second-order

texture is a more attractive means of improving classification accuracy of optical digital imagery in this forest classification application.

The window size used in deriving first and second order texture derivatives can have a substantial impact on the classification accuracy. Marceau et al. (1990) reported that window size accounts for as much as 90% of the classification variability, using 20 x 20 m SPOT HRV imagery of agricultural and mixed-wood landcover. Their study suggested that no single geometric window size can be applied to account for all cover types that may be captured in a digital image. If the window size is too small, the pattern of most classes will not be captured, however, if it is too large, pixels from more than one class (scaling boundaries) will be included, both of which will result in poorer classifications (Marceau et al., 1990). Franklin and McDermid (1993), Wulder (1996), and Franklin et al. (1996) successfully utilized semivariograms calculated from image semivariance to estimate the optimal window size for each spectral channel. They showed that window size is particular to: (i) the resolution of imagery being used, (ii) the covertype to which the texture analysis is being applied to, and (iii) the type of information the user is trying to extract from texture data. For example, Wulder (1996) used a semivariogram to determine the optimal geographic window size to use for predicting leaf area. Essentially, the semivariogram finds the average object size for a given area, which in the case of forest cover would be the average crown diameter. By using a window size predicted by semivariance, Wulder (1996) was measuring the texture of individual crowns and/or the shadow cast by individual crowns. While this may be desirable to someone trying to predict leaf area (such as Wulder, 1996), it may not be useful in the case of the user trying to measure or describe the texture of a complete stand. It would be logical to assume that a larger window, wherein multiple trees are included, would produce a measurement of the local texture which would better describe the stand.

2.3.4. Texture for Improved Classification Accuracies

There are numerous examples of image texture analysis being applied to satellite images for the purposes of increasing the classification accuracy in landcover mapping applications. A good example is provided by Franklin and Peddle (1990). They used secondary texture derivatives to improve landcover classification of a SPOT HRV image of Gros Morne National Park, Newfoundland. They reported an average classification accuracy increase of 36% from using spectral data alone (51%) by including texture channels with the spectral channels (87%). Aside from the improvement in classification accuracy, Franklin and Peddle (1990) also made the important conclusion that classes which are homogeneous on the ground are characterized adequately by spectral tone alone; but classes which contain distinct vegetation patterns or are strongly related to structure are significantly improved by using texture. A similar conclusion was made by Ryherd and Woodcock (1996), who stated: *"the addition of texture is most beneficial for scenes in which the desired classes exhibit textural differences."*

The literature on applications of high resolution image texture analysis in forest inventory studies is small and current. Lobo (1997) applied texture in image segmentation procedures as an advanced image pre-processing step prior to classification of scanned airphotos with a 0.14 m pixel size. St-Onge and Cavayas (1997) used semivariance to map the forest structure parameters of crown diameter, stand density, and crown diameter on 1 meter resolution MEIS-II imagery. Recently, (Franklin et al., in press) conducted a exploratory study where digital aerial remote sensing data were analyzed using available (within PCI) image processing methods. In one experiment of this study Franklin et al. (in press) applied second-order texture measures to the same *casi* image of the Fundy Model Forest that was used for this research. Initially, average classification accuracies were not improved by the inclusion of texture until a hierarchical merging approach was adopted. However, the use of texture

improved the classification accuracy of several classes when included with the spectral data. Several non-optimal procedures were used (e.g., small training samples, poor class selection), but the results lead the authors to conclude that the topic of texture analysis for improved classification of high resolution digital imagery was worthy of further study.

2.4 Conclusion

The current method for collecting forest inventory is labor intensive and completed in a cyclical fashion on an average interval of ten years using aerial photography as a basic information source. As commercial use of forests are approaching their sustainable limit, forest managers require inventories at shorter time intervals. The detail level of forest inventory maps currently being used has been difficult to achieve through the classification of satellite imagery. The classification of high spatial resolution multispectral digital imagery has been identified as a possible solution to the requirement of increasing class detail. In the near future, such high spatial resolution digital imagery may be available from satellite platforms, greatly reducing the cost of acquiring this type of data, and making it feasible for use in forest management inventories. Forest managers utilizing high resolution digital imagery will most likely be using commercially available software packages and the classification algorithms inherent to them. Therefore, relatively simple techniques are desired that can improve classification accuracies while using these algorithms.

High spatial resolution data introduces the problem of spectral variability, also referred to as scene noise or the "H-resolution problem". Several ways of dealing with increased spectral variability have been outlined in this chapter, and can be grouped into two broad categories: those that try to eliminate spectral variability, such as individual tree crown delineation, and those that utilize the spectral variability as an information source to be included in the classification procedure, such as texture. While both have their pros and cons, texture

analysis utilizing a second-order texture measure, is available in industry image analysis software packages, and provides a low cost supplemental data source. The degree to which second-order texture measures can improve the classification accuracy of high resolution digital images, while incorporating a classification scheme with a detail level equivalent to that which is currently found on forest inventory maps, will be the focus of this study.

3. STUDY AREA AND DATA COLLECTION

3.1. Location and Description of Study Area

The study area is situated in the Fundy Model Forest (FMF), centered near Petitcodiac, New Brunswick (Figure 3.1). The FMF is a 420,000 hectare working forest that contains towns and villages, industrial freehold land, Crown Land, Fundy National Park, and many small private woodlots. FMF is one of eleven model forests which are part of Canadian and international efforts to develop model forests for the purposes of research (NRC, 1994). Being within the Acadian forest region (Rowe, 1972) the FMF is characterized by a wide variety of forest species and forest conditions. At the study site hardwood species are predominantly red maple (*Acer rubrum* L.), white birch (*Betula papyrifira* Marsh.), and trembling aspen (*Populus tremuloides* Michx.), with yellow birch (*Betula alleghaniensis* Britton.), grey birch (*Betula popufolia* Marsh.), sugar maple (*Acer saccharum* Marsh.), striped maple (*Acer pensylvanicum* L.), white ash (*Fraxinus americana L.*), and beech (*Fagus grandifolia* Ehrh.) also present in smaller quantities. The dominant softwood species are jack pine (*Pinus banksiana* Lamb.), balsam fir (*Abies balsamea* (L.) Mill.), white pine (*Pissodes strobus* L.), and white spruce (*Picea glauca* (Moench) Voss), with some red spruce (*Picea rubens* Sarg.), and red pine (*Pinus resinosa Ait.*). Due to glaciation, the area is underlain with a thick overburden of unconsolidated diamicton (till), resulting in a hummocky topography and erratic drainage patterns. Topographic relief in the area covered by the two images used in this study (section 3.2.1.) is minimal.

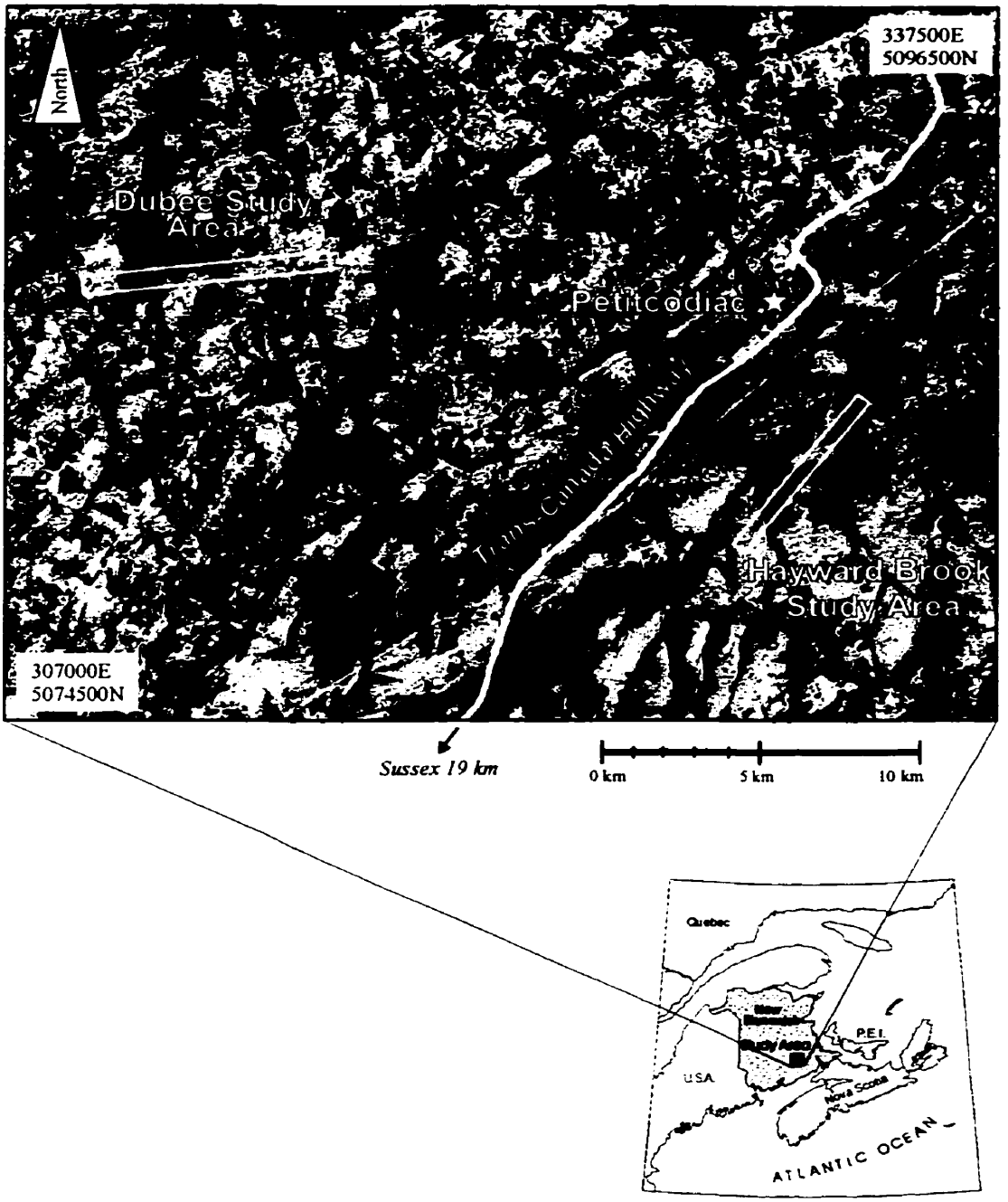

Figure 3.1 TM false color composite (channels 3, 4, 5) of study area. Pink areas are agricultural, natural grasslands, or new cut-overs, and green areas are predominately forested. Location of individual *casi* flight lines are indicated by white rectangular boxes and described in section 3.2.1.

3.2. Data Acquisition

Two types of data must exist before a classification project can be executed. (i) ground observation data and (ii) imagery of the corresponding area. A physical data set was collected on the ground at points spread over the entire study area. This information was used to construct detailed stand descriptions for each point. Imagery for this study is composed of a Compact Airborne Spectrographic Imager data set, which is a high spatial resolution digital image. The following sections will provide a detailed description of the ground and image data sets.

3.2.1. Compact Airborne Spectrographic Imager (casi)

The Compact Airborne Spectrographic Imager or *casi* is a compact, pushbroom type imaging sensor that can be mounted in lightweight aircraft allowing for the acquisition of high spatial resolution (≤1m) digital multispectral imagery (Wulder et al., 1996b). Being a "pushbroom" style sensor, the *casi* utilizes both the aircraft elevation above ground and forward velocity to determine pixel size. It can record spectral information between the range of 430 nm to 870 nm with a possible sampling interval of 1.8 nm (Wulder, 1996). The *casi* was the first commercially available airborne spectrographic imager that was programmable, allowing the user to customize each mission (Lillesand and Kiefer, 1994). The versatility of the *casi* has made it an attractive sensor to researchers and as a result it has been utilized in a wide range of forestry applications (e.g., Gong, et al., 1992; Franklin and McDermid, 1993; Franklin 1994; Niemann, 1995; Baulies and Pons, 1995; Wulder et al., 1996a; Wulder, 1998b; Franklin et al., in press) and non-forestry related areas, such as fisheries (e.g., Zacharias, et al., 1992; Borstad, et al., 1992).

Due to the cost of acquiring airborne digital imagery, once an image has been acquired it is common practice within the remote sensing community that multiple studies will utilize the

same data set. The *casi* image used in this study was acquired on July 31, 1995, and was initially used in a project by Wulder (1996) with the objective of predicting leaf area. Since the image was acquired three years prior to this project's field campaign, the author did not participate in the image acquisition and therefore only the characteristics of the data set will be described here. For a more complete description of the acquisition of the Fundy Model Forest 1995 *casi* image see Wulder (1996).

The FMF *casi* data set was acquired on July 31, 1995, under favorable atmospheric conditions. The data were atmospherically adjusted and geometrically corrected, using spectroradiometric observations of pseudo-invariant features located throughout the study area (Wulder, 1996). This involved using a spectroradiometer to measure the spectral reflectance of objects on the ground that could also be identified on the image. The spectral difference between the object measured on the ground and its value on the image is the atmospheric interference (assuming the spectral data were measured on the ground at the same time the imagery was being acquired). By removing the difference a simple atmospheric correction of the imagery was performed. The FMF *casi* data set is composed of two flight lines of approximately 8 km each in length, average width of 500 m, with a spatial resolution of 1 m^2, and five bands centered at 565.0, 645.4, 665.1, 711.0, and 750.6 nm, as shown in Table 3.1.

Table 3.1 Fundy Model Forest *casi* image channel summary (after Wulder, 1996)

Channel	Bandwidth (nm)	Centre (nm)	Width (nm)
1 (green)	560.5 - 569.4	565.0	8.9
2 (red)	640.9 - 649.8	645.4	8.9
3 (red well)	660.6 - 669.6	665.1	9.0
4 (red edge)	707.4 - 714.6	711.0	7.2
5 (infrared)	748.8 - 752.4	750.6	3.6

In this study, the two flight lines are referred to as Dubee and Hayward Brook (location shown in Figure 3.1). The Dubee flight line has a wide range of forest cover types including: plantations, naturally regenerating stands, reclaimed farm land, and second and third generation mature stands. In contrast the Hayward Brook flight line is covered entirely by mature stands with the exception of one jack pine plantation (Figure 3.2). On both flight lines active harvesting is in progress and a substantial percentage of the imagery has been cutover. Since the flight lines were recorded at different azimuths, each flight line was treated separate in the training and classification stages.

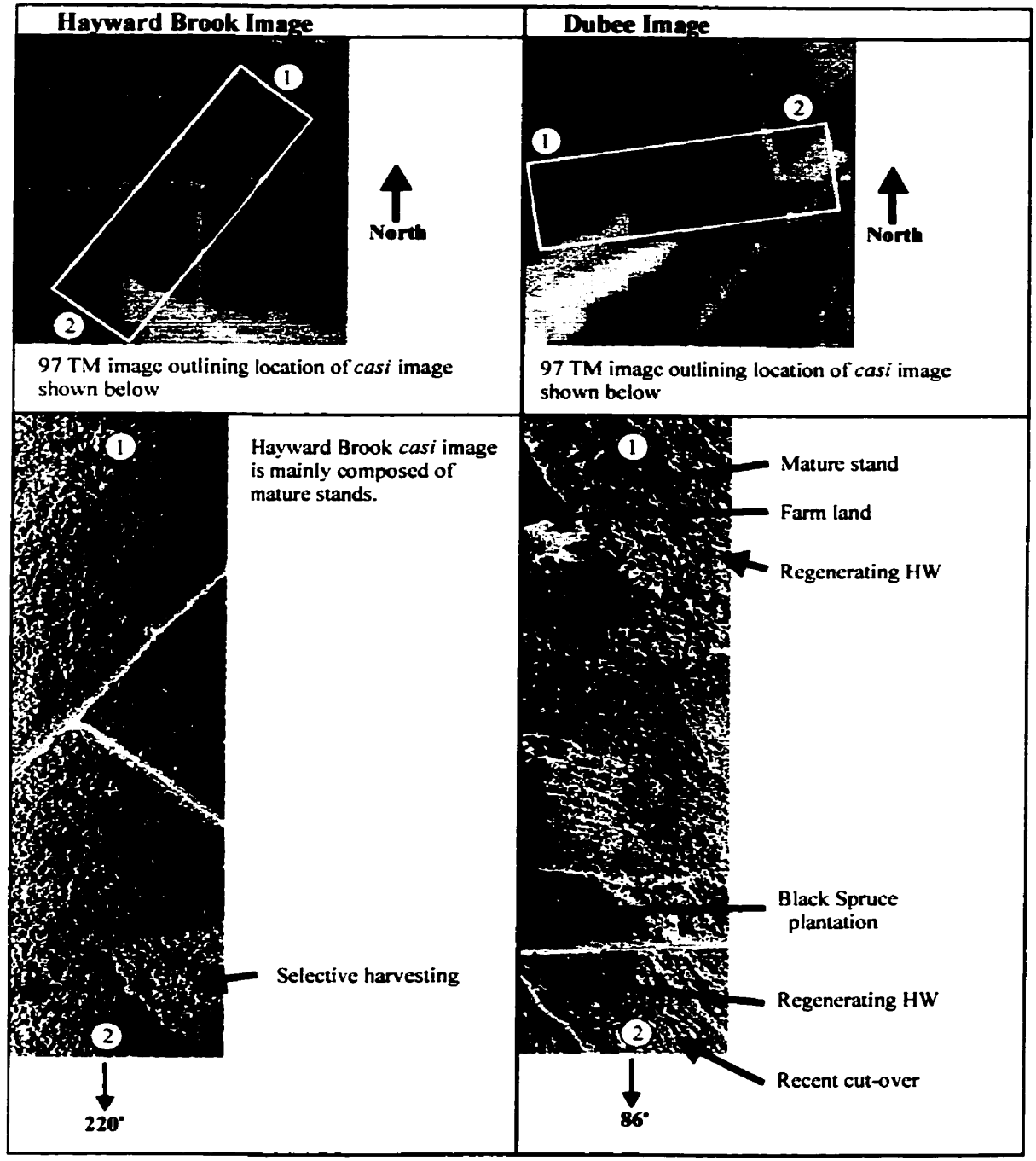

Figure 3.2 Portions of both the Hayward Brook (bottom left) and Dubee (bottom right) *casi* image are shown with the corresponding area of the 1997 Thematic Mapper image (top). All imagery is depicted as a false color composite wherein conifer species appear green, deciduous species pink to red, and roads and new cuts teal.

3.2.2. Ground Based Data

One of the single most important components of this study is the field data. Without a reliable source of ground cover information, training for classification would not be possible, nor would the accuracy of that classification be measurable. While in some cases, observations made from airphotos or information derived from forest stand maps are suitable for training and assessing classification accuracy, due to the level of ground cover detail and accuracy demanded by this study those options were determined to be non-viable. Previously, similar studies have employed a fixed plot or fixed area method of sampling (Franklin and McDermid, 1993; Franklin, 1994; Gerylo et al., 1998), wherein each tree within the area is measured for attributes such as: species type, diameter, height, crown dimensions, and age. Structural information may also be recorded, such as crown closure, stand maturity, and perhaps even biophysical measurements, such as leaf area or photosynthetic capacity. The benefit of fixed area method is that an extremely detailed plot map can be constructed. However, the higher the detail level the greater the time investment and subsequently the smaller the total area that can be observed on the ground. While studies which attempt to predict leaf area (e.g., Wulder et al., 1996a; Franklin et al., 1997; or White et al., 1997) or perform mixture analysis (e.g., Peddle et al., 1999) need highly detailed plot descriptions, for this study a more generalized description of species composition and forest structure is sufficient. As a result, a fixed area plot method of cruising the area corresponding to the imagery would produce an abundance of information at each plot, while minimizing the possible total area mapped. Therefore, a plotless survey method would be more logical for this application.

Plotless cruising or point sampling implementing a prism sweep methodology is a viable alternative to the fixed plot method (Avery, 1967 and Luckai, 1997) and has been used in similar studies (e.g., Martin et al., 1998). In this approach, from a single fixed point trees are counted in or ignored based on their image through a wedge prism. The optical properties

of a prism are such that the bole of the tree appears increasingly offset as one moves away from the tree. That is, the offset through the prism is proportional to the distance from the tree and the diameter of the tree's bole. If the bole of the tree at breast height is completely offset (i.e., two complete stems are visible) the tree is not included in the tally, if the bole through the prism overlaps with the true bole the tree is counted as in, and if it is borderline every other tree is included (Figure 3.3). Therefore, the likelihood of tallying any

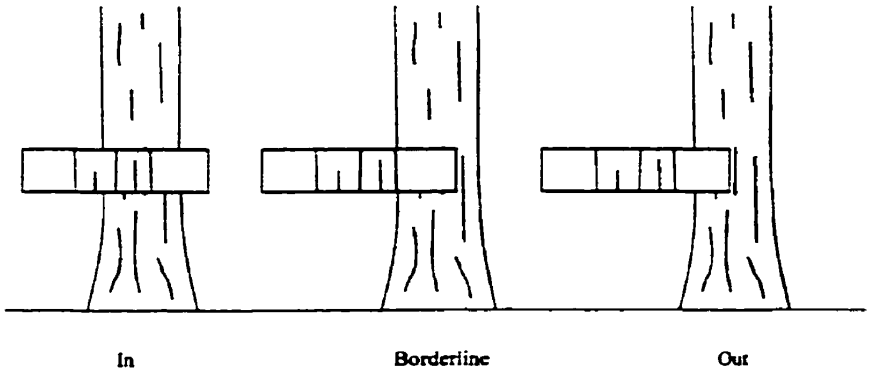

Figure 3.3 Three scenarios encountered when viewing the bole of a tree through a wedge prism. (after Luckai, 1997)

given tree is proportional to its basal area, which is the tree cross-sectional area measured at breast height (Luckai, 1997). This method is ideal for measuring species composition for the purposes of classifying digital imagery, because the greater the tree size, the larger its contribution to the total crown area and subsequently the influence on the measured spectral response.

Prisms can range in Basal Area Factor (BAF) or thickness. The thicker the prism the higher the BAF. BAF (expressed in m^2/ha) can be used to estimate the basal area per hectare by multiplying the number of trees counted in, by the BAF. For example, if the cruiser counted

ten trees in using a BAF of four, the basal area per hectare for that point would be forty. If more than one point was measured in a stand, the basal area per hectare from each point within the stand would be summed, and then divided by the number of points measured to obtain the average basal area per hectare value for the entire stand. Similarly one can also determine the stems per hectare for a stand from the following equation:

$$\text{stems/ha} = \Sigma \frac{\text{BAF} \times 10000}{\text{BAcm}^2} \qquad [1]$$

Where: BA is the basal area for each individual tree counted in the prism sweep calculated as:

$$\text{BA cm}^2 = \left(\frac{\text{dbh cm}}{2}\right)^2 \times \pi \qquad [2]$$

Where : dbh is the tree's diameter at breast height

Stems per hectare allows one to assess the maturity and density of a stand. For example a spruce plantation with tightly spaced trees may yield a stems per hectare value of 3000-5000, whereas a mature spruce stand would most likely have a stems per hectare value of around 500-900. While the species composition of both plots is the same, by utilizing the stems per hectare values it becomes obvious that they should be treated as separate stands.

Field measurements of diameter at breast height (dbh), crown diameter, tree height, height to live crown, crown closure, and tree age were made. Diameter at breast height (or at 1.3 m) was measured using a dendrometer, which in this case was a simple tape measure that converted circumference to diameter (in cm). A procedure for determining the dbh of

"problem trees" such as split stems and trees on a slope was taken from Luckai (1997). Stems that were split at breast height were treated separately, if they were split above breast height they were considered to be a single stem. Leaning trees were measured at right angles to the stem and not horizontal to the ground. Height and height to live crown were estimated using a Suunto clinometer. This device converts angles recorded through a peep-hole into height when the user is a set distance (15 m or 20 m) from the object being measured. A procedure for measurement of trees using a Suunto clinometer was taken from Luckai (1997). Crown diameter was determined using the average of two measurements taken at ninety degrees to each other and following the procedure outlined in Cole (1995). Crown closure was estimated in accordance to procedure outlined by the New Brunswick Department of Natural Resources and Energy (DNRE)(1996), which maintains five tree crown closure classes as shown in Table 3.2.

Table 3.2 DNRE crown closure classes

Crown Closure Class	Percent Closure
1	10 - 30 %
2	30 - 50 %
3	50 - 70 %
4	70 -90%
5	90% +

Tree age was determined using a softwood increment borer following procedure and recommendations outlined in Luckai (1997) and Avery (1967). In addition, the species of each tree was determined using Knopf (1997) and Ritchie (1996) species identification guides for assistance.

The following field photos are examples of two of the forest variables described above. Plate 3-1 and Plate 3-2 are examples of different crown closures. Plate 3-1 shows a fairly open crown that would most likely be classified in group 2 or group 3 (Table 3.2). Plate 3-2 is a good example of a closed crown that would probably be classified as a group 4 or group 5. Plate 3-3 and Plate 3-4 are examples of what different understories look like on the ground. Plate 3-3 is a good example of what would be described on the ground as a heavy fir understory. Plate 3-4 is an example of light understory with no dominant cover type.

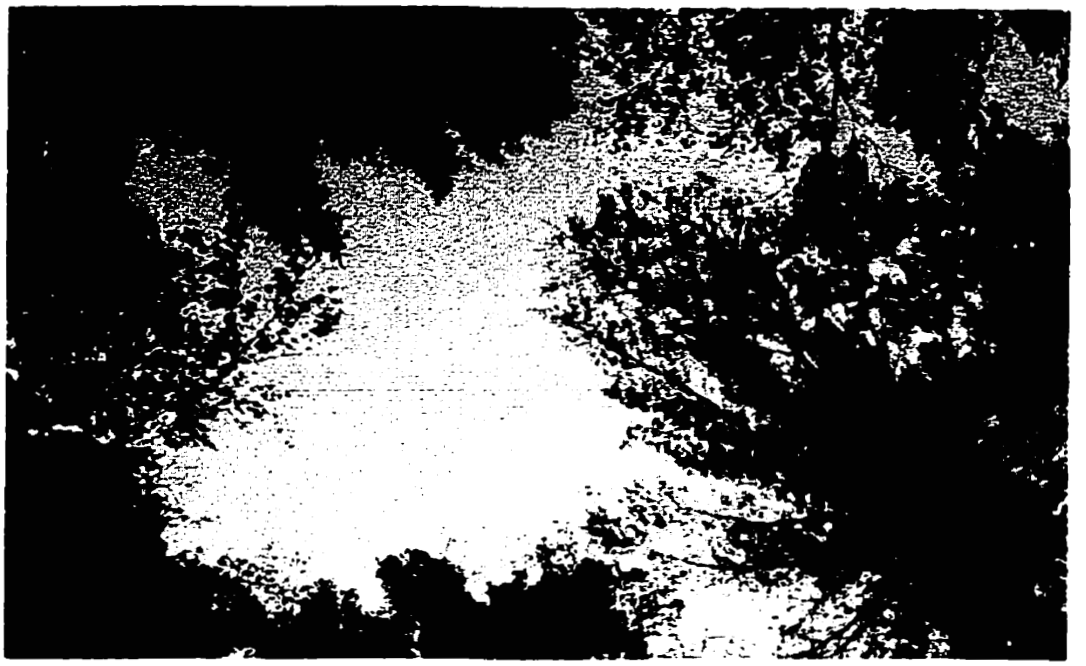

Plate 3-1 Open canopy (low crown closure)

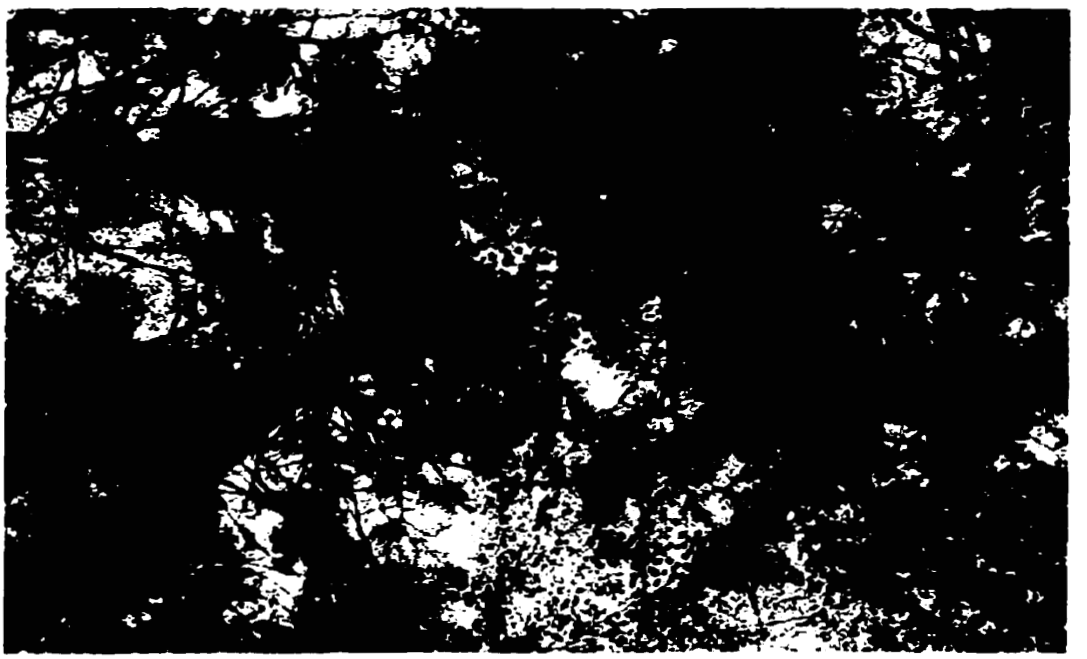

Plate 3-2 Closed canopy (high crown closure)

Plate 3-3 Heavy fir understory

Plate 3-4 Light understory

Due to an onboard power problem in the aircraft that was used during the collection of the *casi* image, GPS data were not collected for each individual line of data. Therefore, the *casi* image could not be geometrically corrected to within an acceptable level of error for this study (5-10 m), and hence a field based GPS could not be used to determine location on the image. As a result a more traditional method of locating ground positions was utilized. This include the use of a Silva Ranger compass for determining directions, a string box (or hip chain) scaled in meters for measuring distance, and a hard copy of the image as well as a 1:15000 topographic map. The scale of the hard copy image was determined from points common to both it and 1:15000 topographic map. Point locations were obtained by following a pre-determined azimuth and distance (never more than 500 m) from a feature of known location (e.g., road intersection, corner of a cutover). All point locations were verified by triangulation and the average positional accuracy is estimated at 5 m $\pm$ 1m.

Between the period of July, 1995 (when the image was acquired) and July, 1998 (when the field data were collected) both flight lines were actively harvested. It was essential to the study to ensure that data retrieved on the ground in 1998 described stands as they were in 1995. Secondly, because of the extremely fine class resolution being used in this study it was imperative that at least two points were collected for any one class, one for training the classifier the other for measuring accuracies. Due to this, a fully random sampling method was not possible, and a modified systematic or regular placement sampling method (utilizing a grid or transect) was employed (Muller et al., 1998). Using this method, forested areas were identified on the image and then later verified on the ground to ensure they had not been altered. Sampling then occurred on a transect with a spacing of 100 meters, and all samples were taken at a minimum distance of 50 meters from any human disturbance. To minimize the effects of sensor look geometry no points were sampled within 100 meters of the edge of the image, thus eliminating areas of extreme shadow or brightness.

At each point visited on the ground a prism sweep was performed using a basal area factor of two at all points. All trees determined in by the prism were measured for diameter at breast height and had their species recorded. A random selection of three trees per point were also measured for height, and crown diameter until a minimum of ten sets of measurements were made for each species making sure to include a large range of dbh. If possible, stand age was recorded from a mature softwood included in the sweep or within the immediate vicinity.

From the crown diameter and tree height measurements bivariate regression analysis was performed to determine the relationship between dbh and height, and dbh and crown diameter for each species (shown in Appendix A and B). Most relationships were either linear or logarithmic with the exception of the Black Spruce height prediction which was best described by a exponential relationship. The dbh vs. height relationship yielded an average r^2 value of 0.68 while dbh vs. crown diameter had an average r^2 of 0.77. Once these relationships were established, tree height and crown diameter were predicted for all trees measured (Appendix C).

Using crown diameter, the percentage of crown per species for each plot was determined, from which the species of each plot was labeled based on its percentage of crown composition. A similar technique was used in Martin et al. (1998), and produces a plot label which is a much better estimate of species composition than using a simple linear relationship between number of stems and species composition (e.g., 8 jack pine stems, 2 white birch = jack pine 80%, white birch 20%), because the crown technique describes the percentage of the forest canopy that each species is contributing to the spectral signature. Once each plot was labeled by species, plots were grouped on each image that had the same species composition, understory descriptor, and similar crown closures and stems per hectare. Two

plots from each group were randomly selected, one to be used for training the classifier and the other for assessing the classification accuracy. As a result of this process twelve groups of plots were selected for use on each image, a total of 48 plots being used.

3.3. Chapter Summary

The Fundy Model Forest, situated in the Acadian forest region, is represented by a wide variety of forest species, forest conditions, and land use. This chapter has described forest species and location of the study area as well as some of its physical qualities. The characteristics and collection methods of the image and field data sets have been outlined.

Chapter 4 will outline the methods which utilize both the imagery and field data sets in a digital classification and the subsequent accuracy assessment. It will also describe the procedure for extracting, quantifying, and utilizing the inherent texture of the imagery, in the classification procedure with the hypothesis that this approach will improve classification accuracies.

4. METHODOLOGY FOR MULTISPECTRAL CLASSIFICATION USING TEXTURE

4.1. Introduction

Most digital image classifications can be grouped into two broad categories: supervised and unsupervised. Supervised classification requires the image analyst to select training areas for each class to be mapped. From the training areas, signatures are generated which act as numerical "identification keys" that describe the statistical attributes of each class. In an unsupervised classification the training stage is removed and the classification algorithm aggregates the images pixels into natural statistical groupings. The user then has to identify and label each group using ground reference data (Lillesand and Kiefer, 1994). The disadvantage of an unsupervised classification is that while the classes generated are statistically separable, they may be of little significance to the user (Cognalton, 1991). If the user has identified the desired classes prior to the classification, such as in this study, a supervised classification is more suitable. A number of modified approaches have been developed over the years to handle specific classification problems where either supervised or unsupervised approaches are not optimal.

The overall goal of any supervised classification is to automatically categorize all pixels in an image to user defined land cover classes. To do this, both spectral and spatial pattern recognition can be used. Spectral pattern recognition relies on different objects or land covers producing different values of pixels based on the spectral reflectance of that feature. In actuality, it does not recognize spectral "patterns" in the geometric sense, but rather it references individual pixels to a set of radiance measurements obtained in user defined spectral bands from each training area. Spatial pattern recognition categorizes image pixels based on their spatial relationship with surrounding pixels and includes geometric shape, size,

and pattern in the decision rule (Lillesand and Kiefer, 1994). The spatial pattern of the pixel values of an object or cover type produces a texture which is unique to that feature.

Image texture analysis is a means of measuring or recognizing the spatial pattern inherent to high resolution multispectral imagery. As demonstrated in the literature review (sub-section 2.3.4.), texture can improve classification accuracy when it is included in a classification procedure. Second-order texture measures are readily available in commercial image analysis software packages, and have even out performed more advanced measures, such as semivariance, when using optical imagery (Carr and Pellon de Miranda, 1998). While there is merit in studies that focus on furthering our understanding of which texture measure is ideal for a given data type, or which attempt to create new and innovative ways of measuring image texture, the objective of this study is to determine to what degree readily available second-order texture measures will improve the classification accuracy of high spatial resolution multispectral digital imagery in a forest inventory classification.

Second-order texture measures require the user to identify five different control variables, those being: window size, the algorithm(s), input channel (i.e., spectral channel to measure the texture of), quantization level of output channel (8-bit, 16-bit, or 32-bit), and the spatial component (i.e., the interpixel distance and angle during co-occurrence computation). Assuming seven algorithms are available, six different spectral channels, window sizes ranging from 3x3 to 21x21 (ten different sizes), three quantization levels, and four possible directions (spatial component), the result would be more than 5,000 different possible combinations that could be used to generate texture channels (i.e., 5000+ would have to be generated). Obviously exploring all of these possible combinations is beyond the scope of this thesis. Finding the optimal set of variables to use in second-order texture analysis of high resolution imagery is not the objective of this study. Therefore, recommendations from previous

literature which attempted to identify these optimal variables will be used as guidelines in conjunction with a small survey made on the image data set used in this study.

4.2. Classification Procedure

The following section will outline the classification procedure used in this study and is broken down into five sub-sections:

1) creation of normalized difference vegetation index (NDVI) channel
2) creation of texture channels
3) signature generation
4) classification
5) accuracy assessment

The methodology for field data analysis was outlined in section 3.2.2.. That analysis produced classes for individual plots based on their species composition and structure, which will be used in the classification of the imagery. The classes are outlined in Table 4.4 (section 4.2.3.)

4.2.1. Creation of Normalized Difference Vegetation Index Channel

Vegetation indices, such as the normalized vegetation difference index (NDVI), defined as:

$$NDVI = (IR\ channel - R\ channel) / (IR\ channel + R\ channel) \qquad [3]$$

were initially developed as a means of detecting the presence and condition of green leaf biomass (Tucker, 1979). NDVI channels have also proven useful at reducing the effects of changing illumination conditions found within in an image caused by differences in surface

slope and aspect to the sun (Mather, 1987). While this study has no intentions of estimating green leaf biomass, or dealing with problems associated with differing levels of solar irradiance, the creation of an NDVI channel provides an additional spectral channel which when included in signature generation is anticipated to increase class separability and hence classification accuracy. Again, the NDVI channel can be readily computed using available software packages and therefore is likely to be used operationally by those attempting forest inventory from digital imagery.

An NDVI channel was created by using the EASI/PACE task of rationing transformation or RTR (PCI, 1997), and input channels 5 (Infrared) and 2 (Red). The calculation was written to a 32-bit real channel and then linearly scaled to an 8-bit channel so that statistics generated from the NDVI channel could be compared to the other spectral channels.

4.2.2. Creation of Texture Channels

As previously mentioned, the use of the grey-level co-occurrence method (second-order texture analysis) requires the user to make several decisions regarding the variables directly associated with it. Marceau et al. (1990) found that the window size used to generate texture channels accounted for as much as 90% of the variability in classification accuracy (ranging from 5x5 to 49x49). Although their study used a SPOT image of an agricultural and mixed-wood land cover, their findings can be taken into consideration when using high spatial resolution imagery because their classes were much broader and therefore probably included a similar amount of texture to that found in detailed classes of high spatial resolution imagery. They also concluded that on average the algorithm used accounted for 7% of the variability in classification accuracy (using: angular second moment, contrast, inverse difference moment, and entropy), and the quantization level only accounted for 3% (16-bit or 32-bit).

Marceau et. al (1990) used the SPOT near-infrared (790 - 890 nm) channel because it exhibited the most contrast (spectral variability) between different land covers. For the spatial component they chose a distance between pixels of one (i.e., neighboring pixel) and the average of the four main interpixel angles (0°, 45°, 90°, and 135°), referred to as directional invariance or invariant (PCI, 1997). Therefore, Marceau et al. (1990) suggest that window size is the factor accountable for the maximum variance in classification accuracy, that the algorithm used plays a minor role, and that the quantization level used is nearly insignificant.

Table 4.1 shows the average standard deviation of pixel values for the five original spectral channels from all 48 plots used in the classification of the Fundy Model Forest *casi* image.

Table 4.1 Mean standard deviation of pixel values for all 48 plots used in the classification.

Channel	Standard Deviation of Pixel Values
1 - green (560.5 - 569.4 nm)	4.17
2 - red (640.9 - 649.8 nm)	2.07
3 - red well (660.6 - 669.6 nm)	1.63
4 - red edge (707.4 - 714.6 nm)	7.99
5 - infrared (748.8 - 752.4 nm)	11.63

The greatest variability in pixel values, or range is found in the infrared channel. Since the infrared channel contains the greatest spectral variability it is logical to assume that it will also contain the most texture (spatial variation in tones). Therefore, the infrared channel was used for all texture analysis. The texture analysis module (TEX) of PCI's (1997) EASI/PACE package was used for second-order texture analysis. This package recommends a quantization level of 32-bit and a spatial component of invariant (mean of all four main

interpixel angles) with an interpixel distance of one. This is in agreement with the findings of Marceau et al. (1990) and was therefore accepted for use in this study.

Two analyses were conducted to determine which window size and algorithm(s) were optimal for the Fundy Model Forest *casi* image. Complete classifications were conducted using ten 18 m radius plots that displayed a wide range of texture. Training and accuracy assessment were conducted on the same plot. This was done for control purposes, to ensure that the only variables introduced were the window size or algorithm(s) selected, and was conducted with the knowledge that assessing the accuracy of training areas will typically produce favorable results. Forty-eight texture channels were created using window sizes of 7x7, 9x9, 11x11, 15x15, 19x19, and 21x21, and the algorithms of homogeneity (HOM), contrast (CON), dissimilarity (DISS), mean (MN), variance (VAR), entropy (ENT), angular second moment (ASM), and correlation (COR). The equations for these algorithms are as follows:

$$\text{Homogeneity} = \sum_{j=1}^{n}\sum_{i=1}^{m}\frac{P(i,j)}{(1+[R(i)-C(j)]^2)} \qquad [4]$$

$$\text{Contrast} = \sum_{j=1}^{n}\sum_{i=1}^{m}P(i,j)(R(i)-C(j))^2 \qquad [5]$$

$$\text{Dissimilarity} = \sum_{j=1}^{n}\sum_{i=1}^{m}P(i,j)|R(i)-C(j)| \qquad [6]$$

$$\text{Mean (of } R(i)) = \sum_{j=1}^{n}\sum_{i=1}^{m}R(i)(P(i,j)) \qquad [7]$$

$$\text{Variance (of } R(i)) = \sum_{j=1}^{n}\sum_{i=1}^{m}P(i,j)(R(i)-[\text{mean\_}R(i)]^2) \qquad [8]$$

$$\text{Entropy} = \sum_{j=1}^{n}\sum_{i=1}^{m}(-P(i,j))\ln(P(i,j)), \text{ assuming that } 0(\ln(0)) = 0 \quad [9]$$

$$\text{Angular Second Moment} = \sum_{j=1}^{n}\sum_{i=1}^{m}P(i,j)^2 \quad [10]$$

$$\text{Correlation} = \sum_{j=1}^{n}\sum_{i=1}^{m}\frac{P(i,j)(R(i) - Mean\_R(i))(C(j) - Mean\_C(j))}{\sqrt{(Variance\_R(i))(Variance\_C(j))}} \quad [11]$$

Where: P(i,j) is the spatial co-occurrence matrix element, R(i) is the grey level value for a row, and C(j) is the grey level value for a column (PCI, 1997).

From the forty-eight texture channels, four sets of signatures were generated to test the effect window size had on classification accuracy (Table 4.2). These included two groups of four texture channels picked at random, one group with four spectral channels (green, red, infrared, and NDVI) and four texture channels (HOM, ENT, ASM, COR), and the final group with all eight texture channels. The results from this analysis are contained in Table 4.2., and the general conclusion was that a 19x19 window size appeared to produce the best classification accuracies, regardless of which combination of channels were used.

Table 4.2 Per pixel classification accuracies from an analysis conducted to determine optimal window size for generating texture channels to be used in the classification of the Fundy Model Forest *casi* image.

Channel Groupings	7x7	9x9	11x11	15x15	19x19	21x21
HOM, ENT, ASM, COR	30%	34%	40%	51%	81%	77%
CON, DIS, MN, VAR	43%	50%	58%	72%	86%	83%
4SPEC, 4TEX	44%	49%	53%	62%	77%	75%
8 TEX	44%	52%	61%	79%	91%	89%

A second analysis was conducted to determine which texture algorithm alone produced the best classification results. Eight sets of signatures (one for each algorithm) were generated using texture channels created from the 19x19 window. The results in Table 4.3 show that accuracies range from 36% to 47%.

Table 4.3 Per pixel classification accuracies from an analysis conducted to determine the optimal texture algorithms for classifying the Fundy Model Forest *casi* image.

Algorithm	Accuracy %
Homogeneity	37
Contrast	36
Dissimilarity	37
Mean	47
Variance	43
Entropy	38
Angular Second Moment	40
Correlation	36

The conclusion made from these two analyses was that for the Fundy Model Forest *casi* image a window size of 19x19 produced the highest classification results (on average 44% better that a 7x7 window), and that the texture measure used played a relatively minor role, ranging from poorest at 36% with contrast or correlation alone, to best with mean alone at 47%.

With the knowledge gained from the two analyses described above, and the recommendations of Marceau et al. (1990) and PCI (1997), the eight texture channels created using a 19x19

window were selected for use in the main classification.

4.2.3. Signature Generation

Signature generation is the process wherein the analyst identifies a training area of known cover type on the image, and creates a statistical description of the pixel values from that area. This statistical description (mean, and standard deviation of all pixels in training area, defined as a hyperellipse of probability contours) is then used as a reference with which to compare all pixels in the image. A pixel is then assigned to the class with the most similar statistical signature. Traditionally, the training stage, or signature generation stage involves two steps: first, signatures are generated for each of the desired classes, second, the separability of signatures is tested. A common measure of separability is the Bhattacharyya distance measure, which indicates the probability of correct classification, given the signatures selected (Mather, 1987). If separability between signatures is poor, the training process is repeated (i.e., new signatures are generated), and classes are dropped or combined. One problem with this approach is that the signature generation stage is governed by the separability between signatures, instead of the needs of the map user. This present study is attempting to meet the demands of forest inventory, so signatures which show poor separability can not be eliminated because they are ultimately needed by forest managers, therefore separability assessment was not performed, and all signatures were accepted.

On each image (Hayward Brook and Dubee) twelve pairs of plots were selected that had the same species composition, understory descriptor, and similar crown closures and densities (stems per hectare)(Table 4.4). One plot from each pair was used for signature generation while the other was saved for accuracy assessment (section 4.2.5.). Plots were represented on the image by a bitmap with an approximate radius of 18 m (18 pixels). Those pixels lying

Table 4.4 Group classes and structure

Hayward Brook Image

Group	Class	Crown Closure	Stems/ha	Understory	Midstory
1	JP10	4	5500	-	-
2	TH6 IH2 SW2	2	650	hw	hw
3	WP3 SP2 TH2 IH2	4	800	mw	mw
4	SP7 WP1 HW2	3	1350	mw	-
5	WP5 SP3 HW2	4	900	mw	-
6	JP5 SP3 HW2	2	830	mw	-
7	TH3 IH3 SW4	3	650	mw	-
8	IH7 SW3	3	800	mw	mw
9	IH6 TH3 SW1	3	950	sw	-
10	TH5 IH4 SW1	3	900	mw	-
11	IH6 TH4	4	2100	mw	-
12	IH7 TH3	4	2200	mw	-

Dubee Image

Group	Class	Crown Closure	Stems/ha	Understory	Midstory
18	BS8 BF2	2	550	-	-
19	BS8 BF2	4	1700	-	-
20	SP10	5	800	-	-
21	SP10	5	5700	-	-
22	JP10	4	1300	-	-
23	TH4 IH4 SP2	1	700	sw	-
24	TH5 IH4 bF1	4	300	hw	-
25	IH5 TH5	4	500	hw	-
26	IH5 TH5	regenerating stand, approx. 5 years			-
27	IH5 TH4 SP1	3	2200	mw	-
28	IH9 TH1	3	900	mw	-
29	IH9 TH1	regenerating stand, approx. 3 years			-

Crown Closure		
1 = 10-30%	mw = mixedwood	JP = jack pine
2 = 30-50%	sw = softwood	WP = white pine
3 = 50-70%	hw = hardwood	PI = pine
4 = 70-90%	IH = intolerant hardwood	BS = black spruce
5 = 90% +	TH = tolerant hardwood	BF = balsam fir
		SP = spruce

directly under the bitmap were extracted for signature generation. Three groups of signatures were generated from the twelve plots on each image. The first group used only the six available spectral channels (green, red, red well, red edge, IR, and NDVI), the second used only the eight texture channels, and the third used the three spectral channels of green, IR, and NDVI, combined with the five best texture channels (homogeneity, dissimilarity, entropy, angular second moment, and variance). The third scenario did not use all of the texture and spectral channels (i.e., 14 channels) because previous research with this data set and classifier (Franklin et al., in press) showed that when more than 8 or 9 channels were included in the classification stage that the classifier became "overloaded" and accuracies began to decrease. Because of this the three spectral channels with the most variance were chosen, along with the five best texture channels. Signatures were generated using the class signature generator (CSG) module of EASI/PACE (PCI, 1997).

4.2.4. Classification Procedure

Class signatures provide a numerical summation of the pixel values of a user defined training area. The goal of a per-pixel classification is to determine the class of all unknown pixels. This is done by comparing each individual pixel value to that of all signatures generated. Using a statistically based decision rule the pixel is assigned to the class which it most closely resembles.

The maximum likelihood classifier (MLC) is a commonly used statistical classifier that is readily available in most image analysis packages. PCI's (1997) MLC uses a Mahalanobis minimum distance decision rule which defines the range of each class as a hyperellipse surrounding its mean that is represented by probability contours. Mahalanobis distance is a measure of both the distance between a pixel and the centroid of a class, and the shape and distribution of the membership of each class (Foody et al., 1992). Pixels which fall within the probability contours of only one class are assigned to that class. If a pixel falls within the probability contours of more than one class, the pixel is assigned to the class with the highest corresponding probability, based on the pixels position relative to the probabilities contours of each class (not to the nearest centroid, such as a minimum-distance-to-means decision rule). The user has the option of a null class, whereby if a pixel does not fall inside any hyperellipse it is assigned to the null. However, if the user wants to force the decision rule to classify the pixel, the option of no null class is selected and the pixel will be assigned to the most probable class (i.e., nearest class based on Mahalanobis distance).

Three separate classifications were performed on both the Hayward Brook and Dubee images. The first used only signatures generated from the six spectral channels, the second used only signatures generated from the eight texture channels and the third used a combination of both

spectral and texture channels (green, IR, and NDVI, combined with the five best texture channels: homogeneity, dissimilarity, entropy, angular second moment, and variance). The maximum likelihood classification (MLC) module of EASI/PACE (PCI, 1997) was used to classify the images and the option of no null class was selected. The resulting classifications were written to 8-bit channels.

4.2.5. Classification Accuracy Assessment

The accuracy of digital classifications are traditionally expressed in a per-pixel manner. In a per-pixel accuracy assessment the classification accuracy of a class is examined at a user defined assessment area. At the accuracy assessment area, the class of all pixels is known before the classification is conducted. Following the classification the class of each pixel within the assessment area is compared to its known class and the number of pixels in agreement are reported as the classification accuracy. For example, if 700 pixels of an area known to contain 1000 "spruce" pixels were classified as spruce, the per-pixel accuracy of that class would be 70 % (assuming only one accuracy assessment area existed). The per-pixel accuracy assessment method was originally used with low resolution satellite imagery and has also been applied to high resolution airborne imagery (e.g., Franklin et al., in press; Gerylo et al., 1998; Franklin, 1994).

Using the per-pixel method to assess the classification accuracy of high spatial resolution digital imagery has the disadvantage (in terms of classification accuracy) of not taking the natural character of the imagery into account. For example, in a scene of a forested area, pixels may represent the sunlit portion of the crown, the shadowed portion of the crown, sunlit understory, shadowed understory, and bare soil. Pixels falling in areas of shadow, exposed soil, or sunlit understory (if it is different from the overstory) have a high probability

of being mis-classified. If these areas as a whole make up 40% of the scene, the best per-pixel accuracies that can be expected are 60%, assuming all other pixels are correctly classified. However, one argument for the use of texture is that even these shadow pixels can be correctly classified if the pattern in which they occur is different from another area with shadow pixels but different species.

A second accuracy assessment approach which is straight forward and might be more similar to traditional forestry methods of determining map accuracy is through the use of a per-plot classification accuracy assessment. One way of conducting a per-plot accuracy assessment is to simply assign each plot to the class of which the majority of the pixels in that plot were classified. For example, if 60% of the pixels in the plot were classified as spruce the entire plot would be classified as spruce. Per-plot accuracy assessment then compares the known class of the plot to that determined by the classifier and labels it as either right or wrong. If eight out of twelve plots were correctly classified the per-plot accuracy would be reported as 67%.

For this study both per-pixel and per-plot accuracies were calculated using the techniques described above. Assessment areas were defined using the bitmap encoding (MAP) module of EASI/PACE (PCI, 1997), and were separate from the those areas used for training. Following the per-pixel classification, results were entered into an error matrix, which will be described in Chapter 5.

4.3. Chapter Summary

In this chapter, the texture inclusive procedure for classifying the Fundy Model Forest *casi* image has been outlined. This included a description of how the texture channels were generated and what variables were used in their construction. The signature generation procedure was then outlined, followed by a description of the steps used in the classification of the two *casi* flight lines. Finally, two methods for assessing classification accuracy (per-pixel, per-plot) were described. Chapter 5 will provide a summary of the classification accuracies that resulted from the methods outlined in this chapter. The following chapter will also discuss the classification accuracies achieved by individual classes and attempt to draw conclusions about which combination of channels (spectral alone, texture alone, spectral and texture combined) were optimal for them.

5. CLASSIFICATION OF SPECIES COMPOSITION AND STRUCTURE: RESULTS AND DISCUSSION

5.1. Introduction

The spatial and aspatial accuracies of a map ultimately define its value and utility. While spatial accuracies (e.g., $\pm$ 1 m) are often reported on maps, typically the aspatial accuracies (i.e., non spatial information) are not. Maps such as thematic maps that are designed to communicate aspatial data should not be relied on too heavily by decision makers using them if both the spatial and aspatial accuracies are not reported. Thematic maps constructed from the classification of digital multispectral imagery are subject to spatial and aspatial error. Factors such as the accuracy of the base map or ground control points used to geometrically correct the thematic map control its spatial accuracy. Aspatial errors can be a function of inaccurate ground truth data, poor training techniques of the classifier, input channels that do not contain sufficient information to allow the classifier to make accurate decisions, inabilities of the classifier itself, and/or poor atmospheric correction of the imagery, among other related issues. While its essential to reduce or eliminate all of the possible sources of error listed above, the focus of this study is to improve the information content of input channels used in the multispectral classification.

To test the main objective of this study (that the inclusion of textural information extracted from the imagery will improve forest inventory classification accuracies when included in the classification procedure) two separate images and three combinations of data were used as inputs to the classifier. On both the Dubee image and the Hayward Brook image three classifications were conducted, each using signatures generated from different combinations of input channels. The first classification used signatures generated from only spectral channels, the second used signatures generated from only texture channels, and the third used a combination of spectral and texture channels, as shown in Table 5.1.

Table 5.1 Listing of channel combinations used in the classification of both flight lines

Channel Combination	Channels Used
Spectral alone	green, red, red well, red edge, IR, NDVI
Texture alone	HOM, CON, DISS, MN, VAR, ENT, ASM, COR
Spectral and texture	green, IR, NDVI, HOM, DIS, ENT, ASM, VAR

This chapter will review the resulting classification accuracies by reporting on each image separately. A series of tables and figures will be used to report accuracies followed by a discussion where individual plot cases will be examined to provide examples of where texture analysis did and did not improve classification accuracies as expected.

A commonly used tool for displaying and interpreting classification accuracies is the error matrix. For both images error matrices were constructed. From the error matrices, per-pixel and per-plot accuracies were determined, also a KHAT score for each matrix was calculated. The KHAT statistic, also known as the Kappa Coefficient of Agreement was initially defined by Cohen (1960) (in Hudson and Ramm, 1987) as:

$$\text{KHAT} = \frac{N\sum_{i=1}^{r} x_{ii} - \sum_{i=1}^{r} x_{i+}x_{+i}}{N^2 - \sum_{i=1}^{r} x_{i+}x_{+i}} \qquad [12]$$

where

r = number of rows in the error matrix
X_{ii} = number of observations in row i and column i (on the major diagonal)
X_{i+} = marginal total of row i
X_{+i} = marginal total of column i
N = total number of observations included in matrix

Simply stated the KHAT statistic is a measure of the actual agreement minus the chance agreement (Congalton and Mead. 1983) or as defined by Lillesand and Kiefer (1994):

$$KHAT = \frac{\text{observed accuracy - chance agreement}}{1 - \text{chance agreement}} \qquad [13]$$

Essentially the KHAT statistic indicates to what degree the classification is better than one resulting from random assignment. and is scaled from 0 - 1. For example. a KHAT score of 0.39 means the classification was 39% better than one occurring from chance.

5.2. Hayward Brook Image Classification Results

Each class used in the classification of the Hayward Brook Image is reported in Table 5.2. This includes the initial twelve classes outlined in Table 4.4. and five new classes that resulted from class merging (described in this section).

Table 5.2 Hayward Brook classes and structure

Group	Class	Crown Closure	Stems/ha	Understory	Midstory
1	JP10	4	5500	-	-
2	TH6 IH2 SW2	2	650	hw	hw
3	WP3 SP2 TH2 IH2	4	800	mw	mw
4	SP7 WP1 HW2	3	1350	mw	-
5	WP5 SP3 HW2	4	900	mw	-
6	JP5 SP3 HW2	2	830	mw	-
7	TH3 IH3 SW4	3	650	mw	-
8	IH7 SW3	3	800	mw	mw
9	IH6 TH3 SW1	3	950	sw	-
10	TH5 IH4 SW1	3	900	mw	-
11	IH6 TH4	4	2100	mw	-
12	IH7 TH3	4	2200	mw	-
*13	PI5 SP3 HW2	3	870	mw	-
*14	IH7 TH3	4	2100	mw	-
*15	SW8 HW2	3	1000	mw	-
*16	HW6 SW3	3	725	mw	-
*17	HW9 SW1	3	925	mw	-

* classes resulting from merging

Table 5.3 contains the three error matrices (a,b,c) from the initial classification of Hayward Brook image. Table 5.3a reports on the classification using spectral channels alone. Table 5.3b from texture channels alone. and Table 5.3c from a combination of texture and spectral channels. In the bottom row of each matrix individual per-pixel producer's accuracies are reported, and are expressed as the percentage of pixels correctly classified in the accuracy assessment plot. Errors in producer's accuracies are errors of omission. In the extreme right hand column individual per-pixel user's accuracies are reported. User's accuracies indicate the probability that a pixel classified into a given class actually represents that class on the ground. Errors in user's accuracy are errors of commission. In the bottom right hand corner of the matrix the overall per-pixel accuracy is reported, which is calculated by dividing the sum of correctly classified pixels (values along the top left to bottom right major diagonal) by the total number of accuracy assessment pixels used (sum of pixels from accuracy assessment plots) (Congalton. 1988).

From the error matrix it can be determined which classes were confused by the classifier. For example, in Table 5.3b, the classification using texture alone. 710 pixels in class (column) 12 were mis-classified as class 11 pixels. This indicates that the signatures generated for class 11 and 12 were too similar for the classifier to distinguish between. Classes such as these were considered candidates for merging if they had similar species compositions and structures.

The objective of merging was to increase classification accuracies by reducing confusion between classes, while maintaining as much class definition as possible. On the Hayward Brook image two merging iterations were conducted resulting in a total of three classification levels (Table 5.3 a,b,c represents Level 1). A summary of classification accuracies achieved by each class for each level is shown in Figure 5.1, followed by Table 5.4 which shows the error matrices for Level 2, and Table 5.5. which shows the error matrices for Level 3.

a) Accuracy assessment of Hayward Brooks classificaion. Level 1. using only spectral channels

	Field Survey Data													User's
Class	1	2	3	4	5	6	7	8	9	10	11	12	Total	Accuracy
cass Classification														
1	410	1	36	1	13	14	132	65	114	195	38	85	1104	37.1
2	12	846	9	3	3	7	39	36	19	21	21	14	1030	82.1
3	37	3	87	11	34	15	44	29	15	43		4	322	27.0
4	20	3	299	321	233	237	153	136	95	119	105	4	1725	18.6
5	9	-	119	262	293	116	17	42	19	36	7	-	922	31.8
6	-	-	88	432	352	319	28	114	46	15	7	-	1401	22.8
7	40	74	23	27	27	10	82	31	18	80	19	25	456	18.0
8	7	61	13	6	7	15	43	20	15	27	17	7	238	8.4
9	18	9	48	23	17	47	64	67	66	43	58	25	485	13.6
10	50	-	46	22	24	23	44	28	27	87	6	7	364	23.9
11	129	21	164	45	59	203	182	177	197	249	363	163	1952	18.6
12	253	52	69	7	12	42	175	243	401	220	453	732	2659	27.5
Total	985	1070	1001	1160	1074	1048	1003	968	1032	1137	1094	1066	12858	
Producer's accuracy	41.6	79.1	8.7	27.7	27.3	30.4	8.2	2.0	6.4	7.7	33.2	68.7		29

KHAT= 0.22

b) Accuracy assessment of Hayward Brooks classificaion. Level 1. using only texture channels.

	Field Survey Data													User's
Class	1	2	3	4	5	6	7	8	9	10	11	12	Total	Accuracy
cass Classification														
1	960	-	-	-	-	-	-	-	102	178	-	7	1237	76.8
2	-	1070	-	-	-	-	-	-	-	-	-	-	1070	100.0
3	4	-	211	-	133	29	151	210	56	-	-	-	794	26.6
4	-	-	194	196	339	124	2	96	-	13	-	-	963	20.2
5	-	-	70	612	581	548	100	271	19	-	-	-	2201	26.4
6	-	-	4	341	9	63	-	-	-	-	-	-	417	15.1
7	6	-	271		11	138	654	98	7	26	-	-	1211	54.0
8	-	-	63	12		146	-	99	139	-	-	-	459	21.6
9	6	-	49	-	1	-	-	164	434	-	204	-	858	50.6
10	16	-	139	-	-	-	96	7	30	920	-	-	1208	76.2
11	3	-	-	-	-	-	-	43	228	-	586	710	1570	37.3
12	-	-	-	-	-	-	-	-	17	-	304	349	670	52.1
Total	985	1070	1001	1160	1074	1048	1003	968	1032	1137	1094	1066	12858	
Producer's accuracy	96.4	100.0	21.1	16.8	54.1	6.0	65.2	10.0	42.1	80.9	53.6	32.7		48

KHAT= 0.44

c) Accuracy assessment of Hayward Brooks classificaion. Level 1. using texture and spectral channels.

	Field Survey Data													User's
Class	1	2	3	4	5	6	7	8	9	10	11	12	Total	Accuracy
cass Classification														
1	879	-	-	-	-	-	-	-	33	198	-	-	1110	79.2
2	-	1070	-	-	-	-	-	-	-	-	-	-	1070	100.0
3	-	-	190	-	67	123	246	149	180	-	-	-	955	19.9
4	-	-	189	127	365	181	2	237	-	-	-	-	1101	11.5
5	-	-	77	579	380	642	23	122	1	-	-	-	1824	20.8
6	-	-	3	439	233	82	-	2	-	-	-	-	759	10.8
7	-	-	239		10	4	539	155	-	22	-	-	969	55.6
8	-	-	72	15	19	16	4	67	51	-	-	-	244	27.5
9	-	-	46	-	-	-	-	174	217	-	145	-	582	37.3
10	106	-	185	-	-	-	189	17	148	917	-	-	1562	58.7
11	-	-	-	-	-	-	-	65	401	-	882	567	1895	45.5
12	-	-	-	-	-	-	-	-	1	-	-	499	500	99.8
Total	985	1070	1001	1160	1074	1048	1003	968	1032	1137	1094	1066	12858	
Producer's accuracy	89.2	100.0	19.0	10.9	35.4	7.8	53.7	6.8	21.0	80.7	78.8	46.8		46

KHAT= 0.41

Table 5.3 a,b,c Error matrices for Hayward Brook Level 1

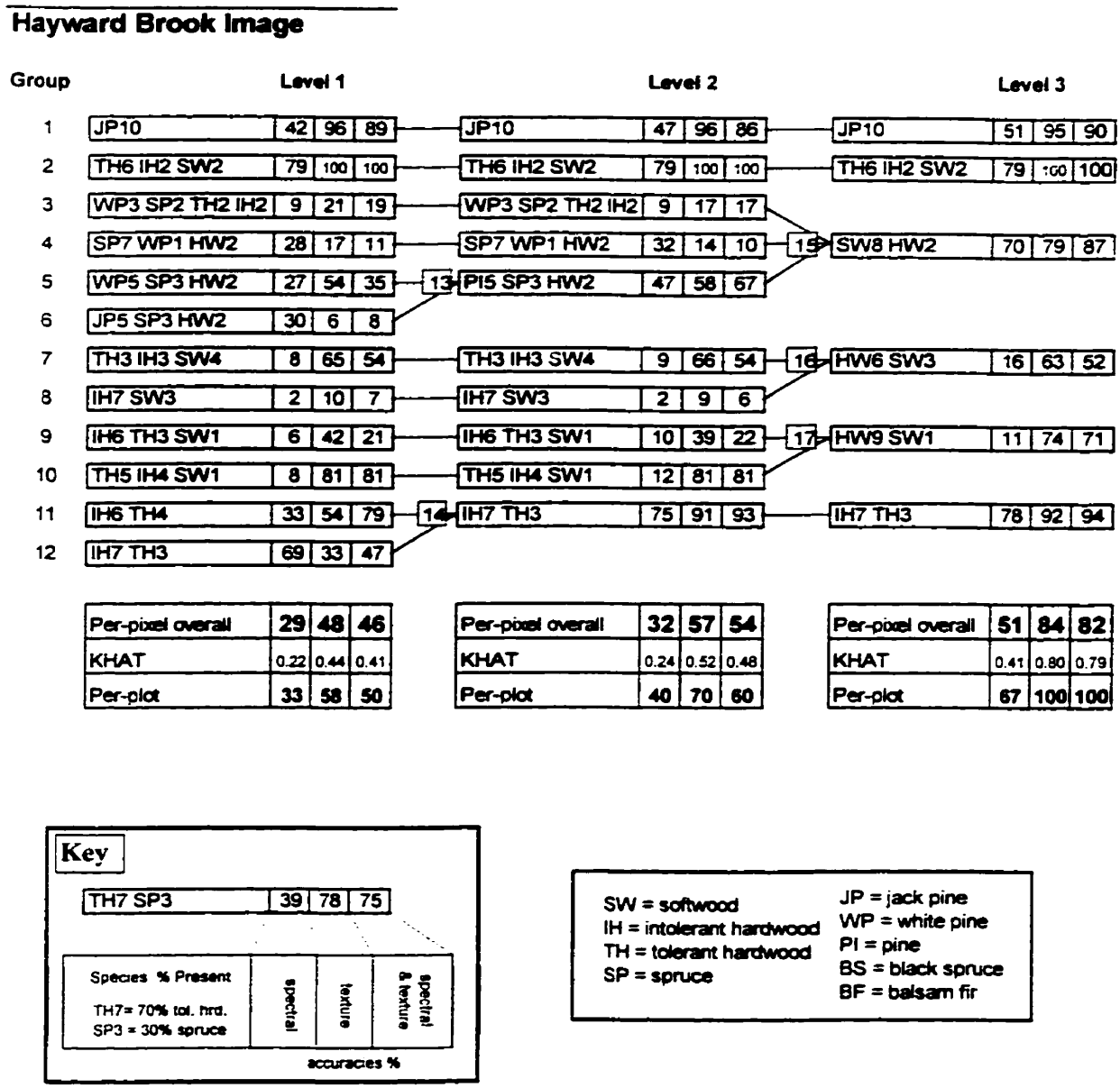

Figure 5.1 Classification results for Hayward Brook classifications. Individual class accuracies are per-pixel producers accuracies.

a) Accuracy assessment of Hayward Brooks classification, Level 2, using only spectral channels.

	Field Survey Data											User's
Class	1	2	3	4	7	8	9	10	13	14	Total	Accuracy
cass Classification												
1	**459**	3	41	1	149	87	135	240	16	80	1211	37.9
2	12	**846**	9	3	39	36	19	21	5	18	1008	83.9
3	38	3	**88**	11	46	37	18	46	30	3	320	27.5
4	20	3	325	**388**	159	154	112	128	270	60	1599	23.0
7	40	80	23	27	**86**	33	18	82	19	22	430	20.0
8	7	61	14	8	47	**19**	16	27	11	11	221	8.6
9	26	14	74	31	98	92	**98**	69	59	67	628	15.6
10	76	-	79	25	59	40	41	**135**	41	10	506	26.7
13	7	-	183	647	32	138	43	46	**486**	5	1599	31.1
14	300	60	165	39	288	352	532	343	112	**804**	2995	26.8
Total	985	1070	1001	1160	1003	988	1032	1137	1061	1080	**10517**	
Producer's accuracy	46.6	79.1	8.8	31.7	8.6	1.9	9.5	11.9	46.9	74.4		32

KHAT= 0.25

b) Accuracy assessment of Hayward Brooks classification, Level 2, using only texture channels.

	Field Survey Data											User's
Class	1	2	3	4	7	8	9	10	13	14	Total	Accuracy
cass Classification												
1	**948**	-	-	-	-	-	83	178	-	-	1209	78.4
2	-	**1070**	-	-	-	-	-	-	-	-	1070	100.0
3	4	-	**167**	-	167	263	57	13	88	-	759	22.0
4	-	-	116	**166**	2	70	-	-	233	-	587	28.3
7	6	-	271	-	**660**	104	7	26	61	-	1135	58.1
8	-	-	59	-	-	**93**	140	-	68	-	360	25.8
9	6	-	49	-	3	178	**400**	-	-	94	730	54.8
10	16	-	137	-	96	7	23	**920**	-	-	1199	76.7
13	-	-	202	**994**	75	241	-	-	**610**	-	2122	28.7
14	5	-	-	-	-	32	322	-	-	**988**	1345	73.3
Total	985	1070	1001	1160	1003	988	1032	1137	1061	1080	**10517**	
Producer's accuracy	96.2	100.0	16.7	14.3	65.8	9.4	38.8	80.9	57.5	91.3		57

KHAT= 0.52

c) Accuracy assessment of Hayward Brooks classification, Level 2, using texture and spectral channels.

	Field Survey Data											User's
Class	1	2	3	4	7	8	9	10	13	14	Total	Accuracy
cass Classification												
1	**848**	-	-	-	-	-	33	198	-	-	1077	78.6
2	-	**1070**	-	-	-	-	-	-	-	-	1070	100.0
3	-	-	**166**	-	262	156	182	-	96		861	19.2
4	-	-	125	**114**	3	205	-	-	238		685	16.6
7	-	-	244	-	**539**	154	-	22	5		964	55.9
8	-	-	65	2	5	**63**	51	-	11		197	32.0
9	-	-	46	-	-	198	**230**	-	-	80	554	41.5
10	106	-	195	-	190	14	149	**917**	-	-	1571	58.4
13	-	-	161	1044	4	163	-	-	**711**	-	2083	34.1
14	33	-	-	-	-	35	387	-	-	**1000**	1455	68.7
Total	985	1070	1001	1160	1003	988	1032	1137	1061	1080	**10517**	
Producer's accuracy	85.9	100.0	16.5	9.8	53.7	6.4	22.3	80.7	67.0	92.6		54

KHAT= 0.49

Table 5.4 a,b,c Error matrices for Hayward Brook Level 2

a) Accuracy assessment of Hayward Brooks classification, Level 3, using only spectral channels.

	Field Survey Data							User's
Class	1	2	14	15	16	17	Total	Accuracy
casi Classification								
1	**506**	10	95	36	156	234	1037	48.8
2	12	**846**	17	4	38	20	937	90.3
14	311	67	**840**	123	350	469	2160	38.9
15	32	3	39	**744**	201	128	1147	64.9
16	57	140	47	89	**155**	115	603	25.7
17	67	4	42	75	96	**119**	403	29.5
Total	985	1070	1080	1071	996	1085	**6287**	
Producer's accuracy	51.4	79.1	77.8	69.5	15.6	11.0		**51**

KHAT= 0.41

b) Accuracy assessment of Hayward Brooks classification, Level 3, using only texture channels.

	Field Survey Data							User's
Class	1	2	14	15	16	17	Total	Accuracy
casi Classification								
1	**931**	-	-	-	-	101	1032	90.2
2	-	**1070**	-	-	-	-	1070	100.0
14	5	-	**989**	-	12	100	1106	89.4
15	-	-	-	**849**	274	9	1132	75.0
16	-	-	-	160	**628**	70	858	73.2
17	49	-	87	62	82	**805**	1085	74.2
Total	985	1070	1080	1071	996	1085	**6287**	
Producer's accuracy	94.5	100.0	91.6	79.3	63.1	74.2		**84**

KHAT= 0.81

c) Accuracy assessment of Hayward Brooks classification, Level 3, using texture and spectral channels.

	Field Survey Data							User's
Class	1	2	14	15	16	17	Total	Accuracy
casi Classification								
1	**889**	-	-	-	-	104	993	89.5
2	-	**1070**	-	-	-	-	1070	100.0
14	33	-	**1014**	-	17	148	1212	83.7
15	-	-	1	**927**	327	20	1275	72.7
16	-	-	-	88	**513**	43	644	79.7
17	63	-	66	56	140	**771**	1096	70.3
Total	985	1070	1080	1071	996	1085	**6287**	
Producer's accuracy	90.3	100.0	93.9	86.6	51.5	71.1		**82**

KHAT= 0.79

Table 5.5 a,b,c Error matrices for Hayward Brook Level 3

On the Hayward Brook image (Figure 5.1) three levels of merging resulted in average overall per-pixel accuracies of 84% when using signatures generated from texture channels alone. On average, the use of texture improved overall per-pixel accuracies 26% and per-plot accuracies 29% over accuracies achieved using spectral channels alone. There were three instances in Level 1 where individual class accuracies were highest using spectral channels alone (classes 4, 6, and 12) and these will be reviewed in more detail in section 5.4. By Level 2, there was only one class that achieved the highest accuracies with spectral channels alone (class 4), and by the third level there were no cases where spectral channels alone outperformed classifications that used texture. On average the use of texture improved KHAT scores 0.30 or 30% over using spectral channels alone.

5.3. Dubee Image Classification Results

Table 5.6 contains a description of the species composition and structures of the classes used in the Dubee image classification. Figure 5.2 contains a summary of the Dubee image classification results. The error matrices for Dubee Level 1 are displayed in Table 5.7, and for Dubee Level 2 in Table 5.8.

Table 5.6 Dubee classes and structure

Group	Class	Crown Closure	Stems/ha	Understory	Midstory
18	BS8 BF2	2	550	-	-
19	BS8 BF2	4	1700	-	-
20	SP10	5	800	-	-
21	SP10	5	5700	-	-
22	JP10	4	1300	-	-
23	TH4 IH4 SP2	1	700	sw	-
24	TH5 IH4 bF1	4	300	hw	-
25	IH5 TH5	4	500	hw	-
26	IH5 TH5	regenerating stand, approx. 5 years			-
27	IH5 TH4 SP1	3	2200	mw	-
28	IH9 TH1	3	900	mw	-
29	IH9 TH1	regenerating stand, approx. 3 years			-
*30	TH4 IH4	4	400	hw	-

* classes resulting from merging

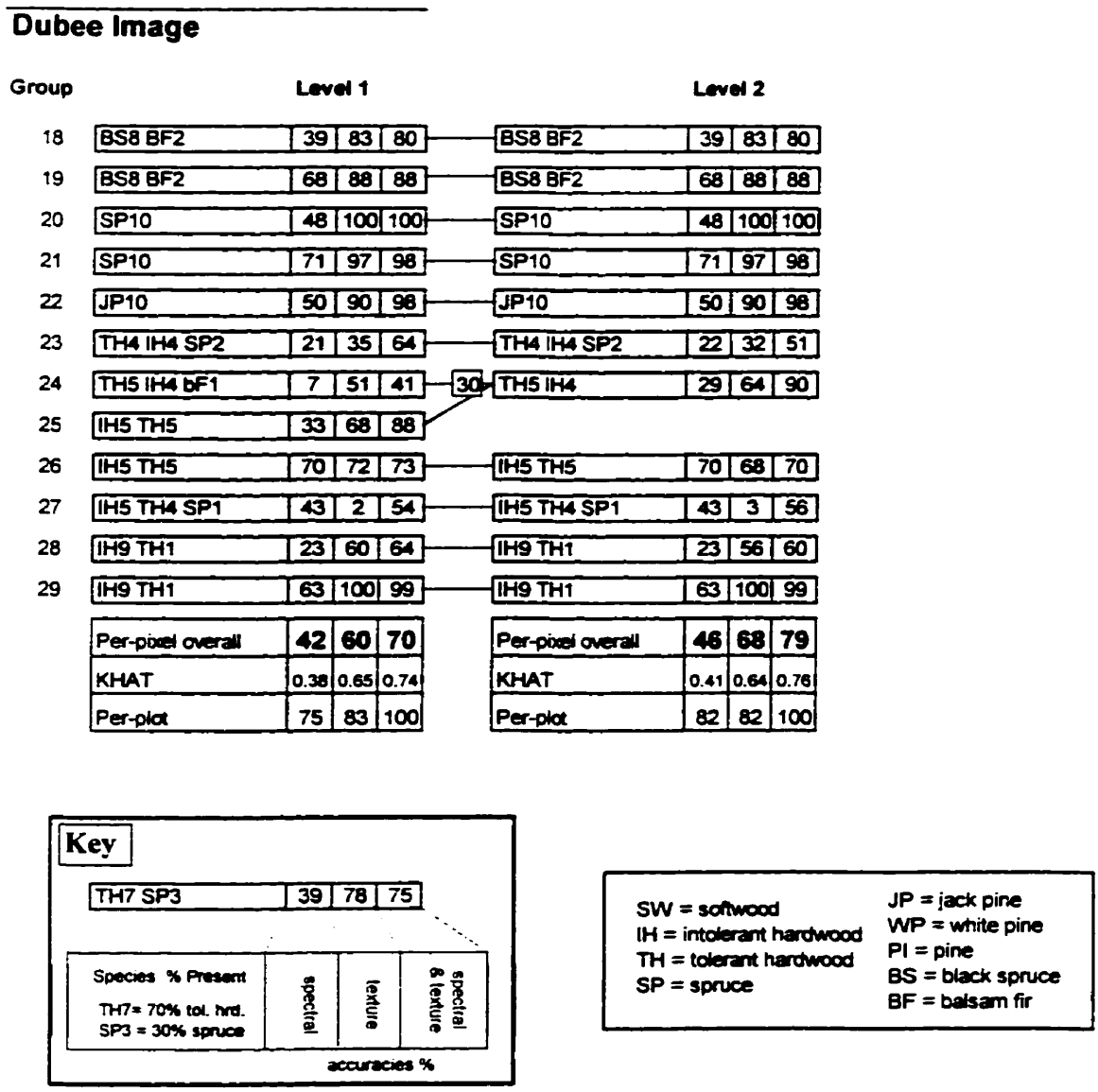

Figure 5.2 Classification results for Dubee classifications. Individual class accuracies are per-pixel producers accuracies.

a) Accuracy assesment of Dubee classification, Level 1, using only spectral channels

Class	Field Survey Data												Total	User's Accuracy
	18	19	20	21	22	23	24	25	26	27	28	29		
corr Classification														
18	436	131	9	-	1	11	6	2	1	1		-	597	72.9
19	515	680	120	1	8	27	2	-	1	2	1	-	1357	50.5
20	25	9	498	35	32	54	1	19	-	13	2	-	688	72.4
21	2	6	184	381	180	39	27	49	7	12	5	-	892	42.7
22	-	7	168	74	253	24	4	14	-	4	2	-	550	46.0
23	118	134	26	17	3	230	46	18	10	116	18	7	745	30.9
24	-	-	-	-	-	50	74	74	46	27	25	31	329	22.5
25	1	19	11	6	1	55	134	292	27	19	19	2	586	49.8
26	-	-	-	3	-	70	232	175	767	38	280	250	1815	42.3
27	11	13	1	3	-	199	200	40	53	468	296	72	1381	35.7
28	1	10	16	14	28	179	105	102	50	82	288	26	881	30.4
29	-	-	-	-	-	155	216	112	134	337	228	663	1845	35.9
Total	1108	1019	1033	534	508	1090	1049	897	1098	1144	1144	1051	11673	
Producer's accuracy	39.3	67.7	48.2	71.3	50.0	21.1	7.1	32.6	69.9	43.1	23.4	63.1		42

KHAT = 0.38

b) Accuracy assessment of Dubee classification, Level 1, using only texture channels

Class	Field Survey Data												Total	User's Accuracy
	18	19	20	21	22	23	24	25	26	27	28	29		
corr Classification														
18	919	121	-	15	22	-	-	-	-	-	-	-	1077	85.3
19	189	898	-	-	-	-	-	-	-	-	-	-	1087	82.6
20	-	-	1033	-	-	-	-	-	-	-	-	-	1033	100.0
21	-	-	-	819	27	-	-	-	-	-	-	-	846	96.1
22	-	-	-	-	457	-	-	-	-	-	-	-	457	100.0
23	-	-	-	-	-	382	210	165	22	20	-	-	799	47.8
24	-	-	-	-	-	214	538	107	67	318	22	-	1264	42.4
25	-	-	-	-	-	469	113	610	10	-	-	-	1222	49.9
26	-	-	-	-	-	-	87	5	791	723	13	-	1619	48.9
27	-	-	-	-	-	-	14	-	119	28	428	-	589	4.6
28	-	-	-	-	-	5	89	10	7	54	681	-	846	80.5
29	-	-	-	-	-	-	-	-	82	1	-	1051	1134	92.7
Total	1108	1019	1033	534	508	1090	1049	897	1098	1144	1144	1051	11673	
Producer's accuracy	82.9	88.1	100.0	97.2	90.3	35.0	51.1	68.0	72.0	2.4	59.5	100.0		80

KHAT = 0.65

c) Accuracy assessment of Dubee classification, Level 1, using spectral and texture channels

Class	Field Survey Data												Total	User's Accuracy
	18	19	20	21	22	23	24	25	26	27	28	29		
corr Classification														
18	883	170	-	7	-	-	-	-	-	-	-	-	1060	83.3
19	225	899	-	-	-	-	-	-	-	-	-	-	1124	80.0
20	-	-	1033	-	-	-	-	-	-	-	-	-	1033	100.0
21	-	-	-	534	10	-	-	-	-	-	-	-	544	98.1
22	-	-	-	3	498	-	-	-	-	-	-	-	499	99.4
23	-	-	-	-	-	696	49	35	17	63	-	-	860	80.9
24	-	-	-	-	-	172	429	60	152	319	40	-	1172	36.6
25	-	-	-	-	-	218	413	786	1	-	-	-	1417	55.4
26	-	-	-	-	-	-	64	-	799	90	-	10	963	83.0
27	-	-	-	-	-	-	15	-	57	612	365	-	1049	58.3
28	-	-	-	-	-	4	79	17	-	57	738	-	893	82.6
29	-	-	-	-	-	-	-	-	72	-	-	1041	1113	93.5
Total	1108	1019	1033	534	508	1090	1049	897	1098	1144	1144	1051	11673	
Producer's accuracy	79.7	88.2	100.0	98.1	98.0	63.9	40.9	87.5	72.8	53.5	64.3	99.0		78

KHAT = 0.74

Table 5.7 a,b,c Error matrices for Dubee Level 1

a) Accuracy assessment of Dubee classification, Level 2, using only spectral channels.

	Field Survey Data												User's
Class	18	19	20	21	22	23	26	27	28	29	30	Total	Accuracy
corr Classification													
18	436	132	9	0	1	11	1	1	-	-	4	594	73.2
19	515	680	120	1	8	27	1	2	1	-	1	1366	50.5
20	25	9	488	35	32	54	-	13	2	-	14	682	73.0
21	2	6	186	381	180	39	7	12	5	-	30	850	44.8
22	-	7	170	74	283	24	-	4	2	-	9	543	46.6
23	118	142	27	16	3	238	11	117	19	7	38	737	32.4
26	-	-	-	3	-	70	767	37	281	246	205	1611	47.6
27	11	13	1	4	-	199	53	469	298	72	124	1255	38.9
28	1	10	16	15	28	180	51	86	267	26	106	786	34.0
29	-	-	-	0	-	153	133	337	228	662	160	1673	39.6
30	1	10	4	5	1	94	74	42	43	36	282	592	47.6
Total	1108	1019	1033	534	506	1090	1088	1144	1144	1051	973	10799	
Producer's accuracy	39.3	67.7	48.2	71.3	56.0	21.9	69.9	43.1	23.3	63.0	29.0		46

KHAT = 0.41

b) Accuracy assessment of Dubee classification, Level 2, using only texture channels.

	Field Survey Data												User's
Class	18	19	20	21	22	23	26	27	28	29	30	Total	Accuracy
corr Classification													
18	919	121	-	15	22	-	-	-	-	-	-	1077	85.3
19	9	898	-	-	-	-	-	-	-	-	-	907	99.0
20	141	-	1033	-	-	-	-	-	-	-	-	1174	88.0
21	-	-	-	519	27	-	-	-	-	-	-	546	95.1
22	-	-	-	-	457	-	-	-	-	-	-	457	100.0
23	39	-	-	-	-	347	10	21	-	-	244	661	52.5
26	-	-	-	-	-	-	743	676	13	-	55	1688	44.0
27	-	-	-	-	-	-	121	36	436	-	7	600	6.0
28	-	-	-	-	-	-	-	65	638	-	47	750	85.1
29	-	-	-	-	-	-	82	1	-	1051	-	1134	92.7
30	-	-	-	-	-	743	142	145	57	-	619	1706	36.3
Total	1108	1019	1033	534	506	1090	1088	1144	1144	1051	973	10799	
Producer's accuracy	82.9	88.1	100.0	97.2	90.3	31.8	67.7	3.1	55.8	100.0	63.6		68

KHAT = 0.64

c) Accuracy assessment of Dubee classification, Level 2, using texture and spectral channels.

	Field Survey Data												User's
Class	18	19	20	21	22	23	26	27	28	29	30	Total	Accuracy
corr Classification													
18	883	120	-	7	-	-	-	-	-	-	-	1010	87.4
19	4	899	-	-	-	-	-	-	-	-	-	903	99.6
20	115	-	1033	-	-	-	-	-	-	-	-	1148	90.0
21	-	-	-	534	10	-	-	-	-	-	-	534	98.1
22	-	-	-	3	486	-	-	-	-	-	-	489	99.4
23	106	-	-	-	-	699	3	81	-	-	49	799	70.1
26	-	-	-	-	-	-	772	101	3	10	26	912	84.6
27	-	-	-	-	-	-	62	637	370	-	1	1070	59.5
28	-	-	-	-	-	-	-	51	699	-	24	785	90.2
29	-	-	-	-	-	-	72	3	-	1041	-	1116	93.3
30	-	-	-	-	-	530	189	271	81	-	873	1944	44.9
Total	1108	1019	1033	534	506	1090	1088	1144	1144	1051	973	10799	
Producer's accuracy	79.7	88.2	100.0	98.1	98.0	51.4	70.3	55.7	60.3	99.0	89.7		79

KHAT = 0.76

Table 5.8 a,b,c Error matrices for Dubee Level 2

On the Dubee image only two levels of merging (Figure 5.2) were necessary to achieve accuracies equivalent to those of the third level of the Hayward Brook image (Figure 5.1). A Level 2 overall per-pixel accuracy of 79% was achieved on the Dubee image using a combination of spectral and texture channels. On average the use of texture improved per-pixel classification accuracies 31% and per plot accuracies 22% over the use of spectral channels alone. There were no instances at the individual class level where the use of texture channels decreased classification accuracies compared to the use of spectral channels alone. The use of texture improved KHAT scores an average of 0.36 or 36%. For the most part, the fact that a combination of texture and spectral channels outperformed texture channels alone can be attributed to the poor performance of class 27 (texture alone). Analysis of the error matrices (Table 5.7b) reveals that 63% of class 27 pixels were mis-classified as class 26 pixels. This suggests that the two classes have very similar textures, and that signatures generated from texture channels alone were too similar for the classifier to distinguish between. Ideally, these two classes, with similar species compositions (Table 5.6) would have been merged, however their structures differ considerably, and therefore remain as separate classes in Level 2. The poor accuracies achieved by class 27 in both levels of the hierarchy using texture channels alone are the main reason that a combination of texture and spectral channels produced the best overall results on the Dubee image.

5.4. Discussion

On average, the use of texture channels improved the per-pixel classification accuracy of the Fundy Model Forest *casi* image by 33%, and per-plot accuracies by 26%, at the lower class detail end of the hierarchies. The purpose of this section is to observe and discuss individual class/plot examples of where texture did and did not work. Out of the initial 24 classes there were only three examples where the use of texture channels decreased classification accuracy. All three of these will be reviewed in Figure 5.3. Figure 5.4 contains examples where the use of texture improved classification accuracies. An effort was made to include examples that covered a wide range of forest cover types.

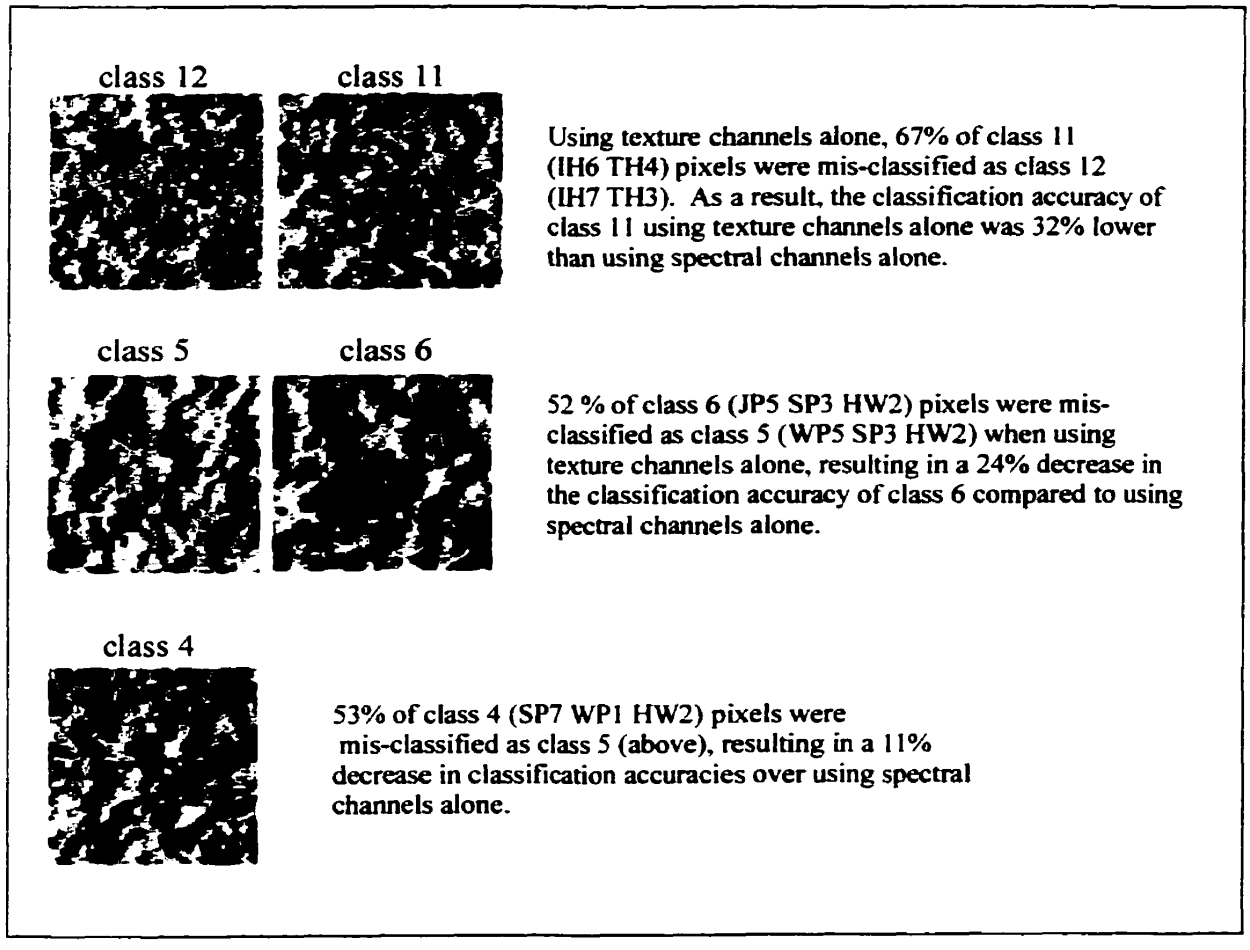

Figure 5.3 The three cases out of twenty four where the use of texture channels resulted in lower classification accuracies than using spectral channels alone.

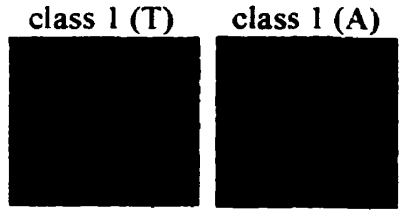

The plot on the left was used for training (T) class 1, which is a jack pine plantation. The plot on the right was used for accuracy assessment (A). With spectral channels alone the per-pixel accuracy of class 1 was 42%, the use of texture channels improved that to 96%.

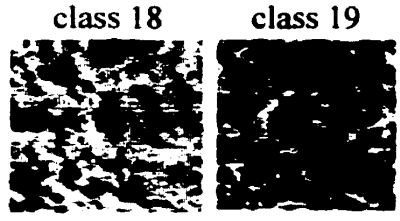

Class 18 and class 19 have the same species compositions (BS8 BF2), but different densities, 550 and 1700 stems/ha respectively. With spectral channels alone 46% of class 19 pixels were mis-classified as class 18, the use of texture reduced that to 17% and improved the classification accuracy of class 19 by 44%.

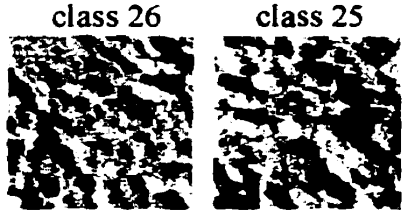

Class 26 and class 25 are both IH5 TH5 stands but class 26 is a regenerating stand whereas class 25 is a mature stand (500 stems/ha). With spectral channels alone 20% of class 25 pixels were mis-classified as class 26, the use of texture reduced that to 0% and improved the classification accuracy of class 25 by 55%.

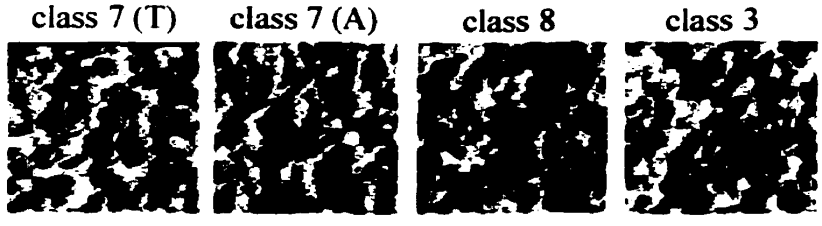

Classes 7, 8, and 3 all have a mixed-wood species composition. With spectral channels alone the classification accuracy of class 7 was only 8%, the use of texture improved that to 65%

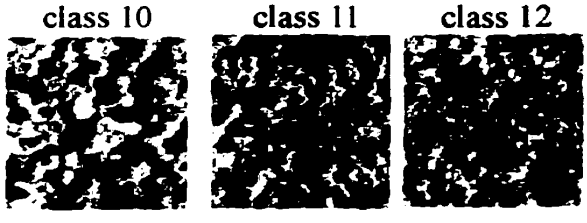

With spectral channels alone 41% of class 10 (TH5 IH4 SW1) pixels were mis-classified as class 11 or 12 (IH6 TH4, and IH7 TH3). Texture reduced that to 0% and increased class 10 accuracies by 73%

Figure 5.4 Examples where the use of texture improved classification accuracies.

Figure 5.3 contains the three examples where the use of texture decreased classification accuracies. In all three cases the individual class that performed poorly with texture was confused predominately with one other class during the classification (class 11 with 12, 6 with 5, and 4 with 5). This suggests that the textures of the two classes being confused were too similar for the classifier to distinguish between. Observation of each of these in Figure 5.3 reveals that all three confused pairs appear to have very similar textures. The failure to separate between these pairs possibly represents a limitation of the texture measure or variables chosen to generate the texture channels, or the classifier itself. However, it also demonstrates the success of the texture inclusive classification procedure used in this study as well as the methods used to collect field data and assign classes to individual plots. For example classes 11 and 12 have identical structures (c.c. 4, stems/ha 2100, understory - mw) and similar species compositions. It would therefore be logical to assume that they should produce very similar textures. The 67% mis-classification of class 11 pixels as class 12 is evidence of this.

The failure of the classifier to separate between classes with similar textures suggests that the classes could be combined. Results of this merging can be observed in Figure 5.1 where class 11 and 12 were combined to form class 14, and classes 4, 5, and 6 are eventually combined in Level 3 to form class 15. As a result, the classification accuracies of these classes using only texture channels was improved an average of 51% from Level 1 to Level 3.

It is also noteworthy to point out that all three cases where texture channels decreased classification accuracy came from the Hayward Brook image. It was anticipated that some classes on both images would perform more poorly with the addition of texture derivatives as the classes were not screened for separability prior to the classification, and all classes were accepted. On the Dubee image several of the classes were predicted to be "texturally

problematic", such as classes 25 and 26 (depicted in Figure 5.4). Although they have different structures (same species composition) the large crowns of class 25 were anticipated to cast very little shadow resulting in a very fine texture similar to that produced by a regenerating stand (e.g., class 26). However, it appears the differences in structure and resulting texture were sufficient for the classifier to distinguish between them, and as a result the use of texture improved the accuracy of all classes.

Figure 5.4 contains several examples where the inclusion of texture channels improved classification accuracies. In the first example, class 1 (jp10), the only plantation class on the Hayward Brook Image was anticipated to have a high classification accuracy with spectral channels alone. However, even at Level 3 (Figure 5.1) the highest accuracy achieved by class 1 was 51%. While it appears that the spectral signature generated from class 1 was confused with other classes, the texture signature provided an initial classification accuracy of 96%. From this example it should be noted that a very homogeneous texture or lack of texture such as that found in class 1 provides as much information to the classifier as a class containing a very coarse texture (e.g., class 7). There tends to be an assumption made in the literature (e.g., Franklin and Peddle, 1987; Marceau et al., 1990) that texture analysis is more beneficial to classes that exhibit a high degree (i.e. coarse) of texture. This may not be true of all classifications, and as class 1 and the examples in Figure 5.3 have demonstrated, texture analysis is most useful when the texture between classes is different, regardless of the level of texture within each class.

The examples of classes 18/19, and classes 26/25 (Figure 5.4) are important for forest inventory reasons because forest managers need classification that separate between regenerating stands, natural or planted, and mature stands of the same species composition. Both examples demonstrate that through texture analysis, stand structure information is being

measured and included in the classification process.

Class 7 is a good mixed-wood example where texture improved classification accuracies. Mixed-wood classes have long been problematic to digital classifications of forest cover, and are quite often grouped into one class, which is not suitable for forest inventory. The class 7 example suggests that more detailed mixed-wood classes are possible if texture is incorporated into the classification.

Finally, the class 10 example exhibits the limitations of spectral channels. With spectral channels alone class 10 had a per-pixel accuracy of 8%, and 41% of its pixels were mis-classified as either class 11 or 12. The inclusion of texture channels improved the classification accuracy of class 10 to 81%. While all three classes had similar species compositions, there is an obvious difference between the structures of class 10 (c.c. 3, 900 stems/ha) and classes 11 and 12 (c.c. 4, stems/ha 2100). The information derived from the texture analysis of these different structures was sufficient enough to separate between class 10 and classes 11/12.

The classification accuracies achieved in this study (80% average at the lower class detail end of the hierarchies) are comparable to other land cover mapping studies that have incorporated texture analysis into the classification of low resolution satellite imagery (e.g., Franklin and Peddle, 1990; Marceau et al., 1990). There are few similar applications of airborne image texture in forest inventory classifications. Franklin and McDermid (1993) achieved a 17% increase in the classification accuracies of seven stand volume classes of Alberta lodgepole pine stands by including texture derivatives in the classification procedure. St-Onge and Cavayas (1997) incorporated texture in a more advanced image segmentation method similar to that used by Lobo (1997) to achieve 80% classification accuracies for forest cover and

density classes. A previous texture inclusive classification project (Franklin et al., in press) which also used the Fundy Model Forest *casi* image achieved a maximum per-pixel accuracy of 57% at a fourth level of merging where only three classes remained. Those results were obtained on a much smaller sample of sites with less variability and suggested the more detailed analysis presented in this thesis was required to fully document texture analysis incorporated in forest inventory classification work

5.5. Optimal Accuracies

From the Hayward Brook image it was concluded that the best overall accuracies were achieved using signatures generated from texture channels alone, whereas on the Dubee image signatures generated from a combination of spectral and texture channels produced the highest accuracies. Furthermore, as Figure 5.3 showed there are certain cases where the use of texture channels resulted in a decrease in classification accuracy. From these observations it can be concluded that each class has an optimal set of input channels, whether it is texture channels alone, spectral channels alone, or a combination of spectral and texture channels. For example, Level 3 of the Hayward Brook image (Figure 5.1) achieved a maximum average accuracy of 84% with texture channels alone, however if the optimal set of input channels for each class is used to calculate the classification accuracy an average of 86% is obtained. Table 5.9 contains the optimal per-pixel classification accuracies for the Hayward Brook and Dubee images. On average, optimal accuracies were 3% better than accuracies generated by using one set of input channels for the entire image. While this is a rather insignificant increase, the concept of having class specific input channels should not be ignored because it is only logical to assume that not every class used in the classification will be best characterized by one set of input channels.

Table 5.9 Optimal per-pixel classification accuracies for the Hayward Brook and Dubee images

Hayward Brook Image		
Level 1	Level 2	Level 3
55 %	60 %	86 %
Dubee Image		
Level 1	Level 2	
72 %	81 %	

5.6. Summary

The fifteen classifications of high resolution multispectral digital data performed in this study showed that on average the use of second-order texture derivatives, included in forest inventory classification improved per-pixel classification accuracies 28%, per-plot accuracies 25%, and KHAT scores 32% over those that used spectral channels alone. At the lower class detail end of the hierarchies an average per-pixel accuracy of 82%, per-plot of 100%, and a KHAT score of 0.78 were achieved. On the Hayward Brook image, texture channels alone produced the highest accuracies but on the Dubee image a combination of spectral and texture channels achieved the highest accuracies. Several individual class examples of where texture did and did not work were examined. The conclusion drawn from these examples was that texture channels did not improve the classifiers ability to separate classes when the apparent texture between two classes was very similar. Out of twenty four initial classes there were three instances where the use of texture did not improve classification accuracies.

6. SUMMARY AND CONCLUSIONS

6.1. Summary

The ability to accurately map forest inventory stands through the classification of high spatial resolution ($\leq$ 1m) multispectral digital imagery provides the potential for producing complete inventories at shorter time intervals than the current industry standard of ten years (air photo interpretation) (Franklin, 1994; Leckie et al., 1995). High spatial resolution multispectral imagery will be available from satellite platforms in the near future, making it economically and logistically feasible for use in forest inventories. To date, one of the main objectives of research using airborne high resolution digital data for the purposes of mapping forests, has been to improve the classification or map accuracy to a level which meets or exceeds that currently achieved by aerial photo interpretation techniques, while at the same time retaining a class or labelling scheme with a similar level of detail to that which is currently found on forest inventory maps.

To meet this goal several advanced high spatial resolution digital image classification techniques have been developed, such as: automated image segmentation (e.g., Ryherd and Woodcock, 1996; Lobo, 1997), pixel un-mixing (e.g., Peddle et al., 1999), and individual tree crown delineation (e.g., Hall et al., 1998). While these methods will undoubtably contribute to the successful use of high spatial resolution image analysis in forestry, there are some disadvantages. For example, they can require extensive field data collection, specialized software not always commercially available to industry, and an advanced understanding of the data and software. Forest managers utilizing high resolution digital imagery in the near future will most likely continue to use commercially available software. Therefore, straight forward and cost effective techniques are desired that can improve the classification accuracy of high resolution multispectral digital imagery

using a forest inventory classification scheme.

This study explored the usefulness of extracting readily available second-order textural information from the high resolution multispectral imagery and including texture in the classification procedure as a supplemental information source to the spectral data. This was done with the hypothesis that texture would increase classification accuracies. In order to meet the needs of forest managers, forest inventory classes outlined by the New Brunswick Integrated Land Classification System (New Brunswick Department of Natural Resources and Energy, 1996) were used in the digital classification.

The Fundy Model Forest study area in southeastern New Brunswick, Canada, provided a wide range of species compositions, stand structures, and stand types. As a result, this allowed for a wide range of classes to be used in the classification. The airborne digital imagery was acquired in July of 1995, and the field data used to train the classifier and assess classification accuracy were collected during June and July of 1998.

Two *casi* images were used for classification. On each image, 12 pairs of plots (one for training, one for accuracy assessment) were selected that had the same species composition, understory descriptor, and similar crown closures and densities. Plots were represented on the image by a circle with an approximate radius of 18 m, creating an average sample size of 1000 pixels. Eight texture channels were generated for each image using the spatial co-occurrence method (Haralick, 1979). Signatures were generated using three different groups of channels. The first used only the six available spectral channels (green, red, red well, red edge, IR, NDVI), the second used only the eight texture channels, and the third used a combination of spectral and texture channels. Three separate classifications were then performed on each image using the maximum

likelihood classifier (no null class). Following the initial classification, confusion matrices were constructed and the signatures of classes that performed poorly (i.e., were confused with other classes) were merged in a hierarchical fashion only if they were similar in species composition and structure.

Using forest inventory classes, the inclusion of second-order texture derivatives in a maximum likelihood classification of high resolution multispectral digital imagery, on average improved per-pixel classification accuracies 28%, per-plot accuracies 25%, and KHAT scores 32%, over classifications that used spectral channels alone. At the lower class detail end of the hierarchies an average per-pixel accuracy of 82%, per-plot of 100%, and a KHAT score of 0.78 were achieved. Out of twenty four initial classes there were three instances where the use of texture did not improve classification accuracies. On one of the images (Hayward Brook) the highest accuracies were achieved using texture channels alone but on the other (Dubee) a combination of texture and spectral channels produced the highest average accuracies. On average, selecting the optimal set of input channels for each class (i.e., spectral alone, texture alone, or spectral and texture combined) improved per-pixel accuracies 3%.

6.2. Conclusions

In the first chapter of this thesis two main objectives were outlined. The results from this research support the following conclusions which are directly related to the two main questions posed in the objectives :

1) - The texture or pattern of the pixel values from a high spatial resolution digital image of forest cover is based on the spectral response characteristics of the stand being depicted. The spectral response and resulting texture of a stand is influenced by species composition and structural characteristics, such as, crown closure, stem density, and understory.

2) - The differences in structure and species composition between forest stands (classes) defined by the New Brunswick Integrated Land Classification System (New Brunswick Department of Natural Resources and Energy, 1996) were large enough to produce unique and statistically separable textures. The inclusion of texture channels derived from readily available second-order texture measures, in a maximum likelihood classification, improved the classification accuracy of twenty one classes out of an initial twenty four.

Several additional conclusions were also made:

- The inclusion of second-order image texture did not improve classification accuracies when two or more classes had very similar species compositions and structures, resulting in similar textures.

- The textural differences between naturally regenerating stands / plantations and mature stands was sufficient to successfully separate between them using second-order texture derivatives.

- The window size used to derive the second-order texture derivatives had a significant impact on the resulting classification accuracies but the algorithms used played a relatively minor role. For this study a limited analysis revealed that a window size of 19 x 19 pixels was optimal.

6.3. Recommendations for Further Research

While answering the questions identified by the research objectives of a study is usually the focus of most research, sometimes the resulting questions and recommendations that the study generates can be as useful as the conclusions drawn. This research as a whole has generated several "questions" or topics which could be the focus of future study. The following list will outline several of the questions raised by this research and also make recommendations to others who wish to use the techniques and methods outlined in this study.

- Window size was identified by this study and others (e.g., Marceau et al., 1990; Franklin and McDermid, 1993) as the single most important texture variable in terms of improving classification accuracy. Optimal window size is a function of the resolution of the imagery being used, the size of the features in the image, and most importantly what type of information the analyst is trying to extract. For example, the window size determined optimal for measuring the texture of a forest stand from a 1 x 1 m digital data set will most likely be non-optimal for someone trying to extract the textural information from an urban landscape using a 10 x 10 m data set. For textural derivatives to be effective the analyst has to ensure that the right information is being extracted.

- This study used a second-order texture measure, which is currently available for use in image analysis packages. While this availability increases the likelihood that it will be used by industry analysts, developing more advanced ways of measuring image texture has the potential to be of great use to not only remote sensing, but all other subjects which attempt to recognize the texture or pattern of digital imagery.

- The classifier used in this study (Maximum Likelihood) makes an assumption of normality (Gaussian) with respect to distribution of the pixel values forming the class training data. Training statistics derived from high spatial resolution digital imagery often contain a wide range of spectral values (from sunlight crown to shadow pixels), as a result classes derived from these stands are typically not statistically normal. This usually leads to a reduction in classification accuracy. While the focus of this study was not to improve classification accuracies through using a more suitable classifier, future classification projects which use high spatial resolution imagery may need to determine if the improvements in classification accuracy achieved in this study can be increased when textural derivatives are combined with a more powerful (or maybe more suitable) classifier.

- While this study has shown the use of texture analysis incorporated in the classification of high spatial resolution multispectral digital images using forest inventory classes is a viable means of improving classification accuracies, the operational logistics of creating a map from the resulting classifications has not been fully considered. Further study may address some of the mapping implications of using high spatial resolution multispectral digital imagery.

7. REFERENCES

Avery, T. E., 1967, *Forest measurements*, McGraw-Hill Book Company, Toronto, ON.

Baulies, F. and X. Pons, 1995, Approach to forest inventory and mapping by means of multi-spectral airborne data. *International Journal of Remote Sensing*, 16(1): 61-80.

Beaubien, J., 1979, Forest type mapping from Landsat digital data. *Photogrammetric Engineering and Remote Sensing*, 45: 1135-1144.

Benson, A. S., and D. S. DeGloria, 1985, Interpretation of Landsat-4 Thematic Mapper and Multispectral Scanner data for forest surveys. *Photogrammetric Engineering and Remote Sensing*, 51: 1281-1289.

Borstad, G., D. Hill, R. Kerr, and B. Nakashima, 1992, Direct remote sensing of herring schools. *International Journal of Remote Sensing*, 13(12): 2191-2198.

Brand, D., 1990, Advances in Canadian forest research: an introduction. *Canadian Journal of Forest Research*, 20: 373-374

Bryant, E., A. G. Dodge, and S. D. Warren, 1980, Landsat for practical forest type mapping: a test case, *Photogrammetric Engineering and Remote Sensing*, 46: 1575-1584.

Bruniquel-Pinel, V., and J. P. Gastellu-Etchegorry, 1998, Sensitivity of high resolution images of forest to biophysical and acquisition parameters, *Remote Sensing of Environment*, 65:61-85

Carr, J. R., and F. Pellon de Miranda, 1998, The semivariogram in comparison to the co-occurrence matrix for classification of image texture, *IEEE Transactions on Geoscience and Remote Sensing*, 36(6):1945-52

Cibula, W. G. and M. O. Nyquist, 1987, Use of topographic and climatological models in a geographical data base to improve Landsat MSS Classification for Olympic National Park, *Photogrammetric Engineering and Remote Sensing*, 53: 67-75

Cohen, J., 1960, A coefficient of agreement for nominal scales. *Education and Psychology Measurement*, 20(1): 37-46

Cole, W. G., 1995, Hardwood tree crown measurement guide, Ontario Forest Research Institute, Sault Ste. Marie, ON

Congalton. R. G., 1991, A review of assessing the accuracy of classification of remotely sensed data. *Remote Sensing of Environment*, 34: 167-178

Congalton. R. G., 1988, A comparison of sampling schemes used in generating error matrices for assessing accuracy of maps generated from remotely sensed data. *Photogrammetric Engineering and Remote Sensing*, 54: 593-600

Congalton. R. G., R. A. Mead, 1983, A quantitative method to test for consistency and correctness in photointerpretation. *Photogrammetric Engineering and Remote Sensing*, 49: 61-74

Congalton. R. G., R. G Oderwald, and R. A. Mead, 1983. Assessing Landsat classification accuracy using discrete multivariate analysis statistical techniques, *Photogrammetric Engineering and Remote Sensing*, 49: 1671-1678.

Connors. R., and C. Harlow, 1980, A theoretical comparison of texture algorithms, IEEE Transactions of Pattern Analysis and Machine Intelligence, 2(3): 204-222

Edwards. G., K. E Lowell, 1995, Modeling uncertainty in photointerpreted boundaries. *Photogrammetric Engineering and Remote Sensing*, 62: 377-391

Franklin. S. E. and D. R. Peddle, 1990, Classification of SPOT HRV imagery and texture features. *International Journal of Remote Sensing*, 11(3): 551-556

Franklin. S. E., and D. R. Peddle, 1987, Texture analysis of digital image data using spatial co-occurrence, *Computers and Geoscience*, 17(8): 1151-1172

Franklin. S. E., and G. J. McDermid, 1993, Empirical relations between digital SPOT HRV and CASI spectral response and lodgepole pine (Pinus contorta) forest stand parameters. *International Journal of Remote Sensing*, 14(12): 2331-2348

Franklin. S. E., 1994, Discrimination of subalpine forest species and canopy density using CASI, SPOT PLA, and Landsat TM data, *Photographic Engineering and Remote Sensing*, 60(10): 1233-1241.

Franklin. S. E., R. H. Waring, R.W. McCreight, W.B. Cohen, and M. Fiorella, 1995. Aerial and satellite sensor detection and classification of Western Spruce budworm defoliation in a subalpine forest. *Canadian Journal of Remote Sensing*, 21(3): 299-308

Franklin, S., M. Wulder, and M. Lavigne, 1996, Automated derivation of geographic windows for use in remote sensing digital image texture analysis, *Computers and Geosciences*, 22(6): 665-673

Franklin, S. E., M. B. Lavigne, M. J. Deuling, M. A. Wulder, and E. R. Hunt, 1997, Estimation of forest Leaf Area Index using remote sensing and GIS data for modeling net primary productivity, *International Journal of Remote Sensing*, 18(16): 3459-3471

Franklin, S. E., R. J. Hall, L. M. Moskal, A. J. Maudie, and M. B. Lavigne, in press, Incorporating texture into classification of forest species composition from airborne multispectral images, submitted to: *International Journal of Remote Sensing*, November, 1998

Gerylo, G., R. J. Hall, S. E. Franklin, A. Roberts, and E. J. Milton, 1998, Hierarchical image classification and extraction of forest species and crown closure from airborne multispectral images, *Canadian Journal of Remote Sensing*, 24(3): 219-232.

Ghitter, G. S., R. H. Hall, and S. E. Franklin, 1995, Variability of Landsat Thematic Mapper data in boreal deciduous and mixed-wood stands with conifer understory, *International Journal of Remote Sensing*, 16(16): 2989-3002

Glackin, D. L., 1998, International space-based remote sensing overview: 1980-2007, *Canadian Journal of Remote Sensing*, 24(3):307 -314

Gong, P., R. Pu, and J. Miller, 1992, Correlating leaf area index of ponderosa pone with hyperspectral *casi* data, *Canadian Journal of Remote Sensing*, 18(4): 275-282.

Gougeon, F. A., 1995, Comparison of possible multispectral classification schemes for tree crowns individually delineated on high spatial resolution MEIS images, *Canadian Journal of Remote Sensing*, 21(1): 1-9.

Hall, R. J., G. Gerylo, and S. E. Franklin, 1998, Estimation of stand volume from high resolution multispectral images, Proceedings, *20th Canadian Symposium on Remote Sensing*, Calgary, AB. 191-196.

Haralick, R., 1979, Statistical and structural approaches to textrue, Proceedings of the IEEE, 67(5): 786-804

Haralick R. M., Shanmugan, K. and Dinstein, I., 1973, Textural features for image classification, *IEEE Transactions on Systems, Man, and Cybernetics*, 3(6): 610-621.

Hay, G. J., K. O. Niemann, G. F. McLean, 1996, An object-specific image texture analysis of H-resolution forest imagery, *Remote Sensing of Environment*, 55: 108-122

Hopkins, P. F., A. L. Maclean, and T. M. Lillesand, 1988, Assessment of Thematic Mapper imagery for forestry applications under lake state conditions, *Photogrammetric Engineering and Remote Sensing*, 54: 61-68

Horler, D. N. H., and F. J. Ahern, 1986, Forestry information content of Thematic Mapper data, *International Journal of Remote Sensing*, 7: 405-428

Hsu, S., 1978, Texture-tone analysis for automated land-use mapping, *Photogrammetric Engineering and Remote Sensing*, 44(11): 1393-1404

Hudson, W. D., 1987, A study to evaluate multispectral imagery digital data for classifying and mapping coniferous forests in the northern Lower Peninsula of Michigan, USA, *Canadian Journal of Remote Sensing*, 13: 39-42

Hudson, W. D., and C. W. Ramm, 1987, Correct formulation of the Kappa Coefficient of Agreement, *Photogrammetric Engineering and Remote Sensing*, 53: 421-422

Irons, J. R., B. L. Markham, R. F. Nelson, J. L. Toll, D. L. Williams, R. S. Latty, and M.L. Stauffer, 1985, The effects of spatial resolution on the classification of Thematic Mapper data, *International Journal of Remote Sensing*, 6(8): 1385-1403

Knopf, A. A., 1997, National Audubon Society field guide to North American trees: eastern regions, Chanticleer Press, Inc., Toronto.

Leckie, D. G., 1990, Advances in remote sensing technologies for forest surveys and management, *Canadian Journal of Forest Resources*, 20: 465-483

Leckie, D., and M. Gillis, 1995, Forest inventory in Canada with an emphasis on map production, *Forestry Chronicle*, 71: 74-88

Leckie, D., J. R. Gibson, N. T. O'Neil, T. Piekutwoski, and S. P. Joyce, 1995, Data processing and analysis for MIFUCAM: a trial of MEIS imagery for forest inventory mapping, *Canadian Journal of Remote Sensing*, 21: 337-356

Lillesand, T.M., and R. W. Kiefer, 1994. *Remote Sensing and Image Interpretation.* Third Edition, John Wiley and Sons, Inc., U.S.A.

Lobo, A., 1997, Image segmentation and discriminant analysis for the identification of land cover units in ecology, *IEEE Transactions on Geoscience and Remote Sensing,* 35(5): 1136-1145

Lowell, K. E. and G. Edwards, 1996, Modeling heterogeneity and change in natural forests. *Geomatica,* 50(4): 425-440

Luckai, F., 1997, Forest measurements field manual. Lakehead University Faculty of Forestry, Thunderbay, ON.

Magnussen, S., 1997, A method for enhancing tree species proportions from aerial photos, *The Forestry Chronicle,* 73(4): 479-487

Marceau, D. J., P. J. Howarth, J. M. Dubois, D. J. Gratton, 1990, Evaluation of the grey-level co-occurrence matrix method for land cover classification using SPOT imagery, *IEEE Transactions on Geoscience and Remote Sensing,* 28(4): 513-517

Martin, M. E., S. D. Newman, J. D. Aber, and R. G. Congalton, 1998, Determining forest species composition using high spectral resolution remote sensing data, *Remote Sensing of Environment,* 65:249-254.

Mather, P. M., 1987, *Computer Processing of Remotely-Sensed Images,* John Wiley & Sons, Inc. UK

Meyer, P., K. Staenz, and K.I. Itten, 1996, Semi-automated procedures for tree species identification in high spatial resolution data from digitized colour infrared-aerial photography, *Journal of Photogrammetry and Remote Sensing,* 51: 5-16

Muller, S. V., D. A. Walker, F. E. Nelson, N. A. Auerbach, J. G. Bockheim, S. Guyer, and D. Sherba, 1998, Accuracy assessment of a land-cover map of the Kuparuk River Basin, Alaska: considerations for remote regions, *Photogrammetric Engineering an Remote Sensing,* 46(6): 619-628.

New Brunswick Department of Natural Resources and Energy (DNRE), 1996, *New Brunswick Integrated Land Classification System,* New Brunswick Department of Natural Resources and Energy, Fredericton, NB, variously-paged.

Natural Resources Canada, 1994, *Model forests, and international network of working models of sustainable forest management*, Ottawa, 43p.

Natural Resources Canada, 1997, *The State of Canada's Forests: Learning from History*, Ottawa, 113p.

Niemann, K. O. 1995, Remote sensing of forest stand age using airborne spectrometer data. *Photogrammetric Engineering and Remote Sensing*. 61(9): 1119-1127

Nelson, R. F., R. S. Latty, and G. Mott, 1984, Classifying northern forests using thematic mapper simulator data, *Photogrammetric Engineering and Remote Sensing*, 50: 607-617

PCI Inc., 1997, EASI/PACE Image Processing System, *User manual*, Version 6.0, Richmond Hill, Ontario.

Peddle, D. R., F. Hall, E. LeDrew, 1999, Spectral mixture analysis and geometric optical reflectance modeling of boreal forest biophysical structure, *Remote Sensing of Environment*, 67(3): 288-297

Ritchie, G. A., 1996, Trees of knowledge: a handbook of maritime trees. Natural Resources Canada, Canadian Forest Service, Fredericton, NB.

Ryherd, S. and C. Woodcock, 1996, Combining spectral and textural data in the segmentation of remotely sensed images, *Photogrammetric Engineering and Remote Sensing*, 62(2): 181-194

Sader, S. A., D. Ahl, and W. Liou, 1995, Accuracy of Landsat TM and GIS rule based methods for forest wetland classification in Maine, *Photogrammetric Engineering and Remote Sensing*, 53: 133-144

Stehman, S. V., and R. L. Czaplewski, 1998, Design and analysis for thematic map accuracy assessment: fundamental principles, *Remote Sensing of Environment*, 64: 331-344

St-Onge, B. A. and F. Cavayas, 1997, Automated forest structure mapping from high resolution imagery based on directional semivariogram estimates, *Remote Senising of Environment*. 61: 82-95

Strahler, A. H., 1980, The use of prior probabilities in maximum likelihood classification of remotely sensed data. *Photogrammetric Engineering and Remote Sensing*. 10: 135-163

Teillet, P. M., B. Guindon, and D. G. Goodenough. 1981. Forest classification using simulated Landsat TM data. *Canadian Journal of Remote Sensing*, 7: 51-60

Holmgren, P. and T. Thuresson. 1998. Satellite remote sensing for forestry planning - a review, *Scandinavian Journal of Forest Research*. 13: 90-110

Tucker, C., 1979, Red and photographic infrared linear combinations for monitoring vegetation, *Remote Sensing of Environment*, 8: 127-150

Walsh, S. J., 1980, Coniferous tree species mapping using Landsat data. *Remote Sensing of Environment*, 9: 11-26

Waring, R., J. Aber, J. Melillo, and B. Moore III, 1986, Precursors of change in terrestrial ecosystems, *Bioscience*, 36(7): 433-438

Weszka, J., C. Dyer, and A. Rosenfeld, 1976, A comparative study of texture measures for terrain classification. *IEEE Transactions of Systems, Man, and Cybergenetics*. 6(4): 269-285

Williams, D. L. and R. F. Nelson, 1986, Use of remotely sensed data for assessing forest stand conditions in the eastern United States. *IEEE Transactions on Geoscience and Remote Sensing*, 24: 130-138

Woodcock, C. E., A. H. Strahler, 1987, The factor of scale in remote sensing, *Remote Sensing of Environment*, 21: 311-332

Wulder, M. A., 1998a, Optical remote-sensing techniques for the assessment of forest inventory and biophysical parameters, *Progress in Physical Geography*. 22(4): 449-476.

Wulder, M. A., 1998b, Image spectral and spatial information in the assessment of forest structural and biophysical data, presented at the *International Forum on Automated Interpretation of High Spatial Resolution Digital Imagery for Forestry*, Natural Resources Canada, Forestry Canada, Pacific Forestry Centre, Victoria, BC.

Wulder, M.. A., 1996, Airborne remote sensing of forest structure: estimation of leaf area index, *Unpublished M.Sc. Thesis*, Department of Geography, University of Waterloo.. ON.

Wulder. M. A., S. E. Franklin, and M. B. Lavigne. 1996a. High spatial resolution optical image texture for improved estimation of forest stand leaf area index. *Canadian Journal of Remote Sensing*, 22(4): 441-449

Wulder. M.., S. Mah, and D. Trudeau. 1996b. Mission planning for operational data acquisition campaigns with the *casi*, presented at the *Second Annual Airborne Remote Conference and Exhibition*, San Francisco, June 23-27, vol. III, pp.53-6.

Zacharias, M., O. Niemann, and G. Borstad, 1992, An assessment and classification of a multispectral bandset for the remote sensing of intertidal seaweeds, *Canadian Journal of Remote Sensing*, 18(4): 263-274

Appendix A Regression plots for diameter at breast height (dbh) vs tree height.

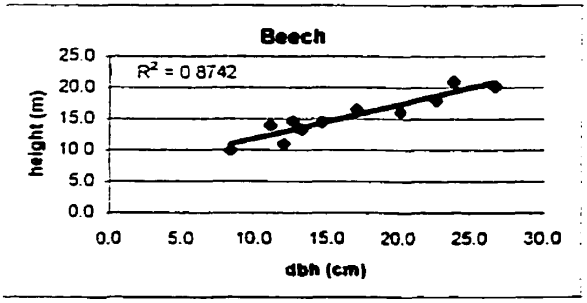

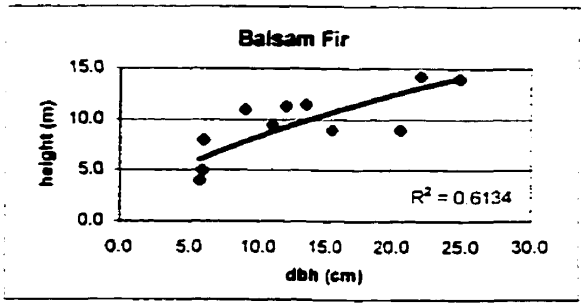

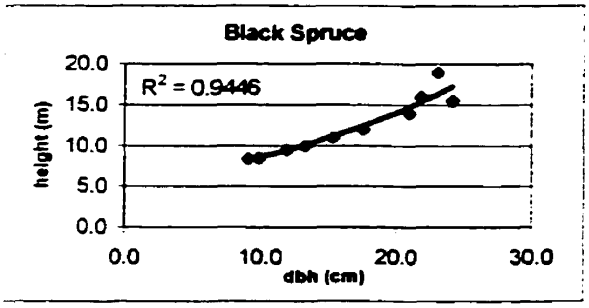

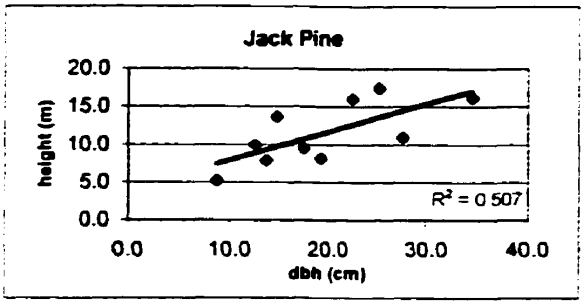

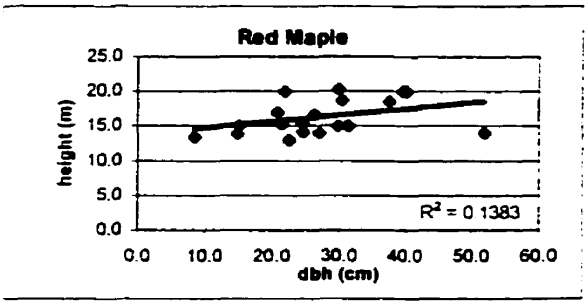

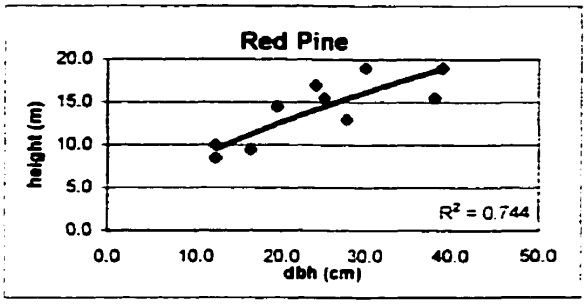

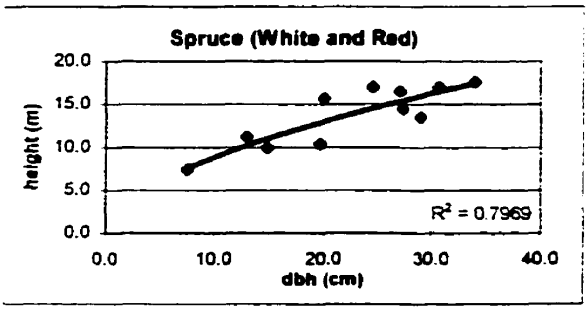

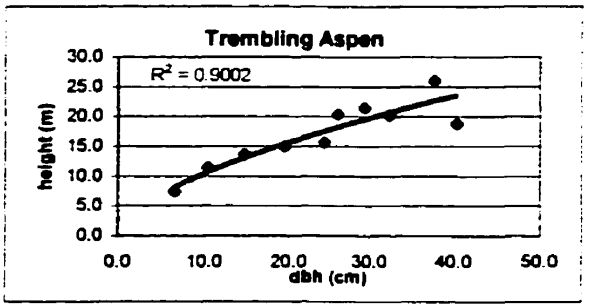

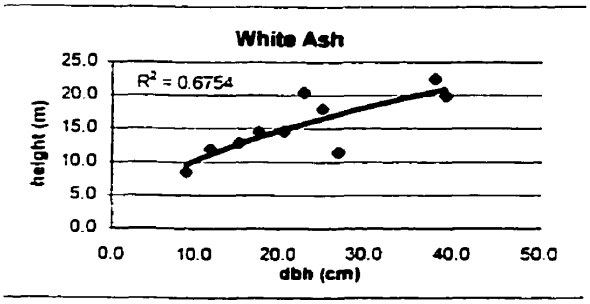
White Ash
R^2 = 0.6754
height (m)
25.0
20.0
15.0
10.0
5.0
0.0
0.0
10.0
20.0
30.0
40.0
50.0
dbh (cm)

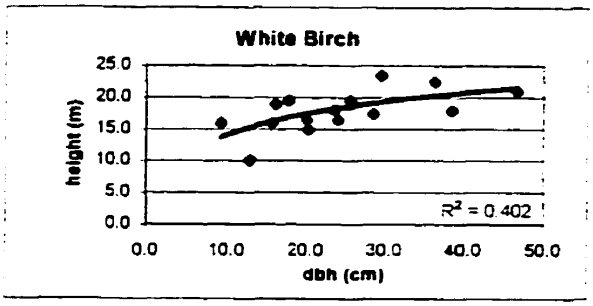
White Birch
height (m)
25.0
20.0
15.0
10.0
5.0
0.0
R^2 = 0.402
0.0
10.0
20.0
30.0
40.0
50.0
dbh (cm)

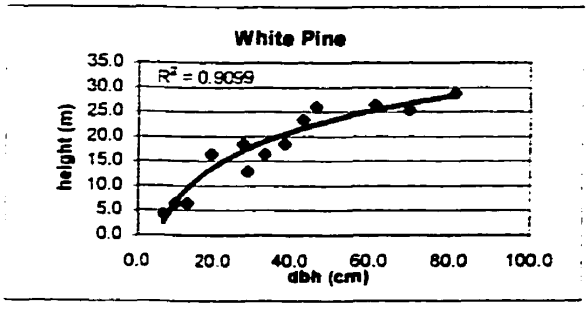
White Pine
R^2 = 0.9099
height (m)
35.0
30.0
25.0
20.0
15.0
10.0
5.0
0.0
0.0
20.0
40.0
60.0
80.0
100.0
dbh (cm)

Appendix B Regression plots for diameter at breast height (dbh) vs crown diameter (cd).

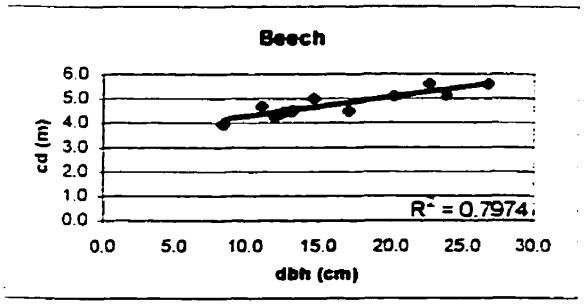

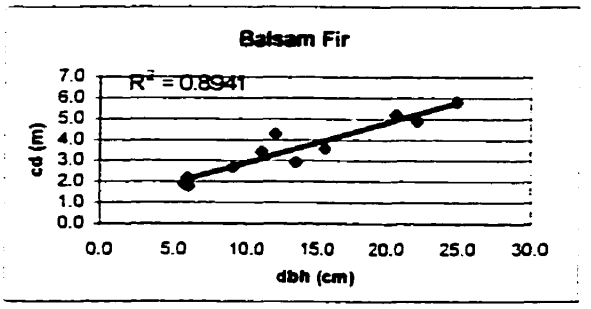

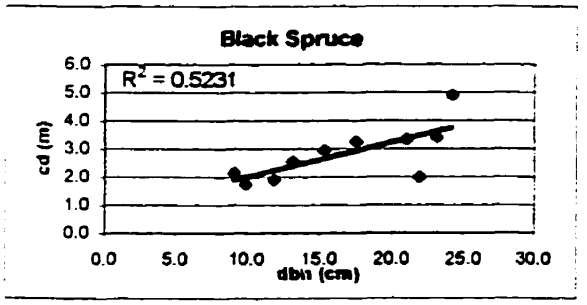

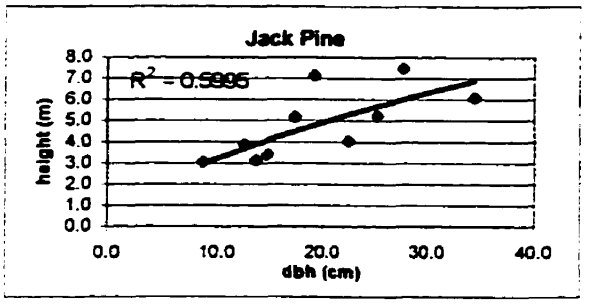

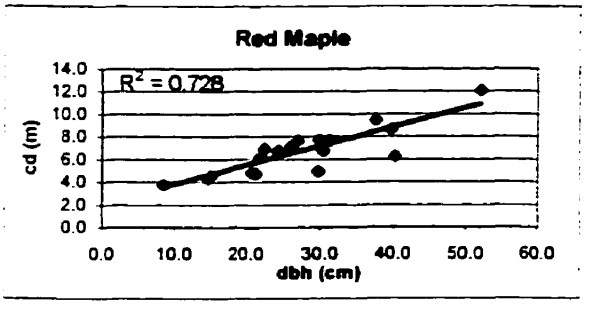

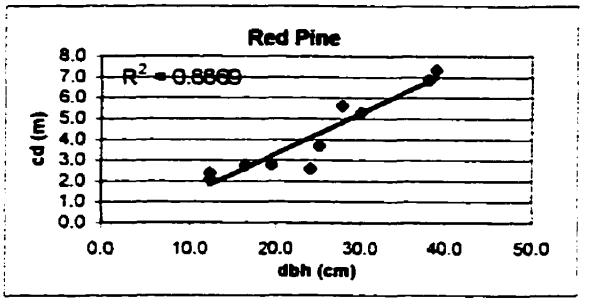

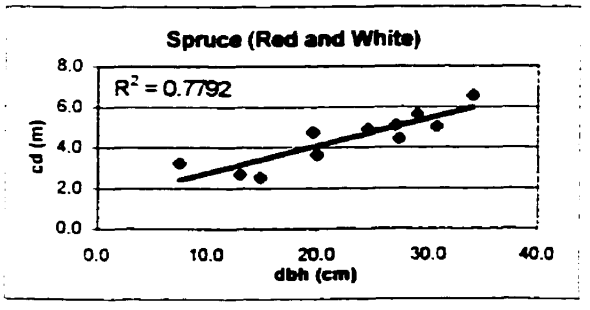

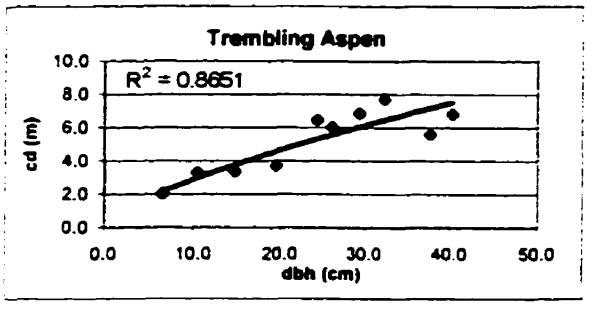

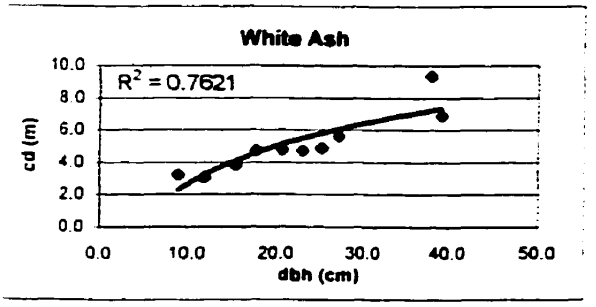
White Ash
$R^2 = 0.7621$
cd (m)
dbh (cm)
0.0
2.0
4.0
6.0
8.0
10.0
0.0
10.0
20.0
30.0
40.0
50.0

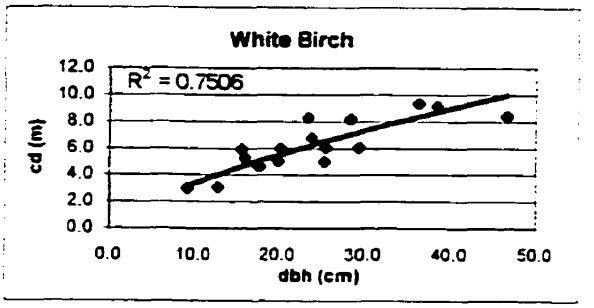
White Birch
$R^2 = 0.7506$
cd (m)
dbh (cm)
0.0
2.0
4.0
6.0
8.0
10.0
12.0
0.0
10.0
20.0
30.0
40.0
50.0

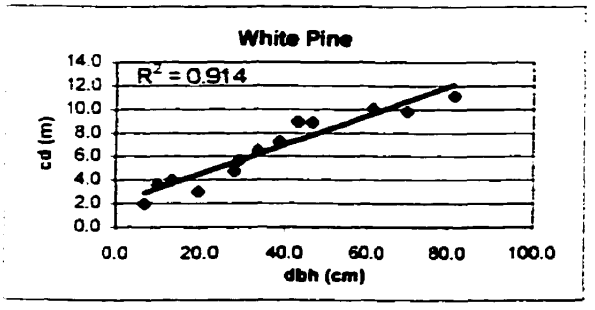
White Pine
$R^2 = 0.914$
cd (m)
dbh (cm)
0.0
2.0
4.0
6.0
8.0
10.0
12.0
14.0
0.0
20.0
40.0
60.0
80.0
100.0

Appendix C Examples of original plot statistics and regressed values for points used in the study.

Dpoint 2 tree #	352P species	205L dbh (cm)	group 28 height (m)	cd (m)	basal area (cm^2)	stem/ha	%crown by species
5	rm	19.9	15.6	5.1	311.0	64.3	14.9
1	rm	19.1	15.5	5.0	286.5	69.8	
4	SP	22.1	13.7	4.4	383.6	52.1	6.5
9	wb	21.9	17.8	5.8	376.7	53.1	78.7
10	wb	26.0	18.7	6.6	530.9	37.7	
8	wb	15.5	16.2	4.6	188.7	106.0	
13	wb	26.6	18.8	6.7	555.7	36.0	
2	wb	19.6	17.3	5.4	301.7	66.3	
6	wb	12.9	10.1	3.1	130.7	153.0	
7	wb	25.5	18.6	6.5	510.7	39.2	
11	wb	18.4	17.0	5.2	265.9	75.2	
12	wb	17.0	16.6	4.9	227.0	88.1	
3	wb	14.8	16.0	4.4	172.0	116.3	
13				67.6		957.1	100.0
soil	m						
cc	3						
slope	0						
mid	none						
und	SPf	30.0	4m				
	stm	30.0	4m				
	litter						

Dpoint4 tree #	207P species	760L dbh (cm)	group 21 height (m)	cd (m)	basal area (cm^2)	stem/ha	%crown by species
1	SP	10.2	8.9	2.8	81.7	244.8	100.0
2	SP	7.0	7.2	2.3	38.5	519.7	
3	SP	15.8	11.4	3.5	196.1	102.0	
4	SP	7.6	7.6	2.4	45.4	440.9	
5	SP	10.6	9.1	2.8	88.2	226.6	
6	SP	10.8	9.2	2.8	91.6	218.3	
7	SP	9.9	8.8	2.7	77.0	259.8	
8	SP	16.5	11.7	3.6	213.8	93.5	
9	SP	11.0	9.3	2.9	95.0	210.5	
10	SP	9.0	8.3	2.6	63.6	314.4	
11	SP	9.3	8.5	2.6	67.9	294.4	
12	SP	15.0	11.1	3.4	176.7	113.2	
13	SP	10.0	8.8	2.7	78.5	254.6	
14	SP	7.2	7.4	2.4	40.7	491.2	
15	SP	7.6	7.6	2.4	45.4	440.9	
16	SP	11.3	9.4	2.9	100.3	199.4	
17	SP	15.0	11.1	3.4	176.7	113.2	
18	SP	12.9	10.2	3.1	130.7	153.0	
19	SP	15.5	11.3	3.5	188.7	106.0	
20	SP	6.1	6.7	2.2	29.2	684.4	
21	SP	9.3	8.5	2.6	67.9	294.4	
21				59.9		5775.2	100.0
soil	m						
cc	5						
slope	0						
mid	none						
und	none						

Dpoint14 tree #	163P species	4569L dbh (cm)	group 26 height (m)	cd (m)	basal area (cm^2)	stem/ha	%crown by species
			no mature overstory				
soil	m						
cc	5						
slope	0						
mid	wb/rm	90.0	5m				
	sw	10.0	3m				
und	none						
Dpoint18 tree #	**335P species**	**5642L dbh (cm)**	**group 27 height (m)**	**cd (m)**	**basal area (cm^2)**	**stem/ha**	**%crown by species**
12	bf	7.8	7.2	2.5	47.8	418.6	3.1
7	rm	12.1	14.9	4.4	115.0	173.9	28.6
13	rm	10.1	14.7	4.3	80.1	249.6	
14	rm	12.9	15.0	4.5	130.7	153.0	
15	rm	15.6	15.2	4.7	191.1	104.6	
16	rm	20.1	15.6	5.1	317.3	63.0	
3	SP	15.6	7.4	3.3	191.1	104.6	8.6
18	SP	16.7	11.7	3.6	219.0	91.3	
1	wb	23.0	18.1	6.0	415.5	48.1	59.7
2	wb	15.5	16.2	4.6	188.7	106.0	
4	wb	15.0	16.0	4.5	176.7	113.2	
5	wb	15.6	16.2	4.6	191.1	104.6	
6	wb	17.2	15.0	6.0	232.4	86.1	
8	wb	11.9	14.9	3.8	111.2	179.8	
9	wb	15.7	16.0	6.0	193.6	103.3	
10	wb	15.6	16.2	4.6	191.1	104.6	
11	wb	10.5	14.3	3.5	86.6	231.0	
17	wb	15.3	16.1	4.5	183.9	108.8	
18				80.4		2544.3	100.0
soil	m						
cc	3						
slope	0						
mid	SPf	15.0					
und	bf	40.0					
	stm	40.0					
age	65						